15. Hideshima T, Chauhan D, Richardson P, Mitsiades C, Mitsiades N, Hayashi T, Munshi N, Dang L, Castro A, Palombella V, Adams J, Anderson KC. NF-κB as a therapeutic target in multiple myeloma. J Biol Chem 2002;277:16639–47.
16. Dewan MZ, Terashima K, Taruishi M, Hasegawa H, Ito M, Tanaka Y, Mori N, Sata T, Koyanagi Y, Maeda M, Kubuki Y, Okayama A, et al. Rapid tumor formation of human T-cell leukemia virus type 1-infected cell lines in novel NOD-SCID/γc^{null} mice: suppression by an inhibitor against NF-κB. J Virol 2003;77:5286–94.
17. Kitajima I, Shinohara T, Bilakovics J, Brown DA, Xu X, Nerenberg M. Ablation of transplanted HTLV-I Tax-transformed tumors in mice by antisense inhibition of NF-κB. Science 1992;258:1792–5.
18. Mori N, Yamada Y, Ikeda S, Yamasaki Y, Tsukasaki K, Tanaka Y, Tomonaga M, Yamamoto N, Fujii M. Bay 11–7082 inhibits transcription factor NF-κB and induces apoptosis of HTLV-I-infected T-cell lines and primary adult T-cell leukemia cells. Blood 2002;100:1828–34.
19. Tan C, Waldmann TA. Proteasome inhibitor PS-341, a potential therapeutic agent for adult T-cell leukemia. Cancer Res 2002;62: 1083–6.
20. Dewan MZ, Uchihara JN, Terashima K, Honda M, Sata T, Ito M, Fujii N, Uozumi K, Tsukasaki K, Tomonaga M, Kubuki Y, Okayama A, et al. Efficient intervention of growth and infiltration of primary adult T-cell leukemia cells by an HIV protease inhibitor, ritonavir. Blood 2006;107:716–24.
21. Cahir-McFarland ED, Davidso DM, Schauer SL, Duong J, Kieff E. NF-kappa B inhibition causes spontaneous apoptosis in Epstein-Barr virus-transformed lymphoblastoid cells. Proc Natl Acad Sci USA 2000;97:6055–60.
22. Collier AC. Efficacy of combination antiretroviral therapy. Adv Exp Med Biol 1996;394:355–72.
23. Collier AC, Coombs RW, Schoenfeld DA, Bassett R, Baruch A, Corey L. Combination therapy with zidovudine, didanosine and saquinavir. Antiviral Res 1996;29:99.
24. Collier AC, Coombs RW, Schoenfeld DA, Bassett RL, Timpone J, Baruch A, Jones M, Facey K, Whitacre C, McAuliffe VJ, Friedman HM, Merigan TC, et al. Treatment of human immunodeficiency virus infection with saquinavir, zidovudine, and zalcitabine. AIDS Clinical Trials Group. N Engl J Med 1996;334:1011–17.
25. Markowitz M, Saag M, Powderly WG, Hurley AM, Hsu A, Valdes JM, Henry D, Sattler F, La Marca A, Leonard JM, Ho DD. A preliminary study of ritonavir, an inhibitor of HIV-1 protease, to treat HIV-1 infection. N Engl J Med 1995;333:1534–39.
26. Kempf DJ, Marsh KC, Denissen JF, McDonald E, Vasavanonda S, Flentge CA, Green BE, Fino L, Park CH, Kong XP, Wideburg NE, Saldivar A, et al. ABT-538 is a potent inhibitor of human immunodeficiency virus protease and has high oral bioavailability in humans. Proc Natl Acad Sci USA 1995;92:2484–88.
27. Andre P, Groettrup M, Klenerman P, de Giuli R, Booth BL, Jr, Cerundolo V, Bonneville M, Jotereau F, Zinkernagel RM, Lotteau V. An inhibitor of HIV-1 protease modulates proteasome activity, antigen presentation, and T cell responses. Proc Natl Acad Sci USA 1998; 95:13120–24.
28. Liang JS, Distler O, Cooper DA, Jamil H, Deckelbaum RJ, Ginsberg HN, Sturley SL. HIV protease inhibitors protect apolipoprotein B from degradation by the proteasome: a potential mechanism for protease inhibitor-induced hyperlipidemia. Nat Med 2001;7:1327–31.
29. Schmidtke G, Holzhütter HG, Bogyo M, Kairies N, Groll M, de Giuli R, Emch S, Groettrup M. How an inhibitor of the HIV-I protease modulates proteasome activity. J Biol Chem 1999;274:35734–40.
30. Gaedicke S, Firat-Geier E, Constantiniu O, Lucchiari-Hartz M, Freudenberg M, Galanos C, Niedermann G. Antitumor effect of the human immunodeficiency virus protease inhibitor ritonavir: induction of tumor-cell apoptosis associated with perturbation of proteasomal proteolysis. Cancer Res 2002;62:6901–8.
31. Pati S, Pelser CB, Dufraine J, Bryant JL, Reitz JMS, Weichold FF. Antitumorigenic effects of HIV protease inhibitor ritonavir: inhibition of Kaposi sarcoma. Blood 2002;99:3771–9.
32. Sgadari C, Barillari G, Toschi E, Carlei D, Bacigalupo I, Baccarini S, Palladino C, Leone P, Bugarini R, Malavasi L, Cafaro A, Falchi M, et al. HIV protease inhibitors are potent anti-angiogenic molecules and promote regression of Kaposi sarcoma. Nat Med 2002;8:225–32.
33. Katano H, Pesnicak H, Cohen JI. Simvastatin induces apoptosis of Epstein-Barr virus (EBV)-transformed lymphoblastoid cell lines and delays development of EBV lymphomas. Proc Natl Acad Sci USA 2004;101:4960–5.
34. Norvir, Ritonavir Product monograph. North Chicago, IL: Abbott laboratories, 1997.
35. Gatti G, Di Biagio A, Casazza R, De Pascalis C, Bassetti M, Cruciani M, Vella S, Bassetti D. The relationship between ritonavir plasma levels and side-effects: implications for therapeutic drug monitoring. AIDS 1999;13:2083–9.

International Immunology, Vol. 21, No. 7, pp. 843–858
doi:10.1093/intimm/dxp050

The analysis of the functions of human B and T cells in humanized NOD/shi-scid/γc^{null} (NOG) mice (hu-HSC NOG mice)

Yohei Watanabe[1,2], Takeshi Takahashi[1], Akira Okajima[1], Miho Shiokawa[1], Naoto Ishii[1], Ikumi Katano[3], Ryoji Ito[3], Mamoru Ito[3], Masayoshi Minegishi[4], Naoko Minegishi[5], Shigeru Tsuchiya[2] and **Kazuo Sugamura[1]**

[1]Department of Microbiology and Immunology and [2]Department of Pediatrics, Tohoku University Graduate School of Medicine, 2-1 Seiryo-cho, Aoba-ku, Sendai 980-8575, Japan
[3]Laboratory of Immunology, Central Institute for Experimental Animals, 1430 Nogawa, Miyamae-ku, Kawasaki 216-0001, Japan
[4]Division of Blood Transfusion, Tohoku University Hospital, 2-1 Seiryo-cho, Aoba-ku, Sendai 980-8575, Japan
[5]Department of Health and Welfare Science, Sendai University, 2-2-18 Funaokaminami, Shibata-machi, Miyagi-ken 989-1693, Japan

Keywords: adaptive immunity, humanized mice, NOG mice, thymus

Abstract

'Humanized mice' are anticipated to be a valuable tool for studying the human immune system, but the reconstituted human immune cells have not yet been well characterized. Here, we extensively investigated the differentiation and functions of human B and T cells in a supra-immunodeficient mouse strain, NOD/shi-scid/γc^{null} (NOG) reconstituted with $CD34^+$ hematopoietic stem cells obtained from umbilical cord blood. In these hu-HSC NOG mice, the development of human B cells was partially blocked, and a significant number of B-cell progenitors accumulated in the spleen. The mature $CD19^+IgM^+IgD^+$ human B cells of the hu-HSC NOG mice could produce IgG *in vivo* and *in vitro* by antigenic stimulation. In contrast, although human T cells with an apparently normal phenotype developed, most of them could neither proliferate nor produce IL-2 in response to antigenic stimulation by anti-CD3 and anti-CD28 antibodies *in vitro*. The positive selection of human T cells in the thymus was sufficiently functional, if not complete, and mainly mediated by mouse class II, suggesting that the human T cells lost their function in the periphery. We found that multiple mechanisms were involved in the T-cell abnormalities. Collectively, our results demonstrate that further improvements are necessary before humanized mice with a functional human immune system are achieved.

Introduction

Recently, human immunity research has increased in momentum, owing largely to accumulating evidence that human immunity can be inferred from animal models. However, the extent to which these models directly reflect the human immune system is still open to question. For example, genetic abnormalities often lead to different phenotypes in different species (i.e. patients with spontaneous mutations in a certain gene and the corresponding gene-disrupted mice), resulting in complicated interpretations about the human immune system (1–3). In addition, different responses to pharmacological reagents developed in animals can result in unexpected adverse effects when they are used for therapeutic treatments (4). Hence, the development of novel model systems in which the human immune system can be functionally studied in a reliable manner without various constraints is desired not only for understanding human immunity but also for improving 'translational' research.

'Humanized mice' have been considered one such model (5–9). For the past two decades, many studies have attempted to graft immunodeficient animals with human tissues or cells (10–12). In particular, the inoculation of human hematopoietic cells or PBMCs has been frequently performed to examine whether even a part of the functional human immune system can be reconstituted. Although various immunodeficient mice, including athymic nude mice (*nu/nu*), C.B.-17 *scid* mice, and NOD/SCID mice, have been used as recipients (10–12), there

Correspondence to: T. Takahashi; E-mail: takeshi-takahashi@mail.tains.tohoku.ac.jp
Received 13 March 2009, *accepted* 1 May 2009
Transmitting editor: K. Yamamoto
Advance Access publication 10 June 2009

seem to be major obstacles to the xenotransplantations. For example, the simple transfer of human PBMCs into such immunodeficient animals results in the failure of stable engraftment, the functional impairment of the donor cells and in some cases the uncontrolled activation of human T cells against mouse tissues (xenogenic graft versus host disease) (13, 14). In addition, when human $CD34^+$ hematopoietic stem cells are transferred, the reconstitution of human immune cells is often incomplete, as revealed by a lack of T-cell development in reconstituted NOD/SCID mice (15). Furthermore, the poor graft survival of human hematopoietic stem cells makes it difficult to perform long-term experiments (16). These limitations have hampered the research on human immune systems in humanized mice.

The recent development of a new immunodeficient strain, however, has opened up the possibility for generating better xenotransplantation systems (5, 6, 16). Disruption of the IL-2R γ chain (γc) produces a mouse strain deficient for B, T, NK and NKT cells since the signalings through γc of multiple cytokines (IL-2, IL-4, IL-7, IL-15, etc.) are indispensable for the development of a wide range of immune cell lineages (17–19). By backcrossing the γc knockout (KO) mice onto the NOD background, which has low endogenous NK activity, and introducing the *scid* mutation, the NOD/Shi-scid-IL-2Rγ $(\gamma c)^{null}$ (NOG) strain was generated (16, 20, 21). As a consequence, NOG mice have almost no functional endogenous immune system. Using NOG or the similar BALB-RAG2/γc double-KO mice, several groups have reported a more efficient and stable reconstitution of human hematopoietic cells than was previously possible, using human $CD34^+$ stem cells from various sources, including bone marrow (BM), umbilical cord blood or peripheral blood immobilized by granulocyte colony stimulating factor (16, 20–22). For example, such humanized mice harbor human $CD34^+$ stem cells in their BM for up to 1 year, and the cells can be serially transferred into new recipients to reconstitute them (16). In addition, apparently normal human B and T cells or their progenitors are found in the spleen or BM, respectively (16, 20, 21), and major subsets of human hematopoietic cells have been successfully developed from these mice (22, 23). Hence, these supra-immunodeficient strains are presently considered the most suitable for reconstituting quasi-human immune systems.

Nevertheless, it is also clear that there is room for improvement in the present humanized mouse technology. For example, upon exogenous antigenic challenge, humanized mice (hu-HSC-NOG mice) produce abundant antigen-specific IgM antibodies, but little antigen-specific IgG (21, 22, 24, 25). This predominant IgM production suggests that only a partial reconstitution of the human adaptive immune system is achieved in the hu-HSC-NOG mice. In the present study, we sought to identify critical cues for recapitulating functional human immunity in hu-HSC-NOG mice, mainly focusing on the differentiation and functions of the human B and T cells upon reconstitution.

Methods

$CD34^+$ hematopoietic stem cells

The cord blood from full-term deliveries was obtained from the Miyagi Cord Blood Bank, following the institutional guidelines approved by the Tohoku University Committee on Clinical Investigations. Some $CD34^+$ cell samples were obtained from the RIKEN Bioresource Center Cell Bank (Tsukuba, Japan). Mononuclear cells were isolated from cord blood by density gradient centrifugation using Lymphocyte Separation Medium (MP Biomedicals, Solon, OH, USA) after removing the phagocytes with Silica (Immuno Biological Laboratories, Takasaki, Japan). The cells were washed and suspended in PBS containing 5% FCS. $CD34^+$ stem cells were obtained by magnetic cell sorting (MACS) (Miltenyi Biotech, Bergisch Gladbach, Germany). Briefly, $CD34^+$ cells were labeled with a biotin-conjugated anti-human CD34 mAb (Serotec, Oxford, UK) after FcR blocking and subsequently with anti-biotin microbeads. The magnetically labeled $CD34^+$ cells were purified twice on LS columns. The usual purity of the $CD34^+$ fraction was >95%. The purified $CD34^+$ cells were cryopreserved in Cell Banker (Juji Field, Tokyo, Japan) at −80°C in a deep freezer until use.

Mice and reconstitution with human stem cells

Six-week-old female NOD/shi-scid/γc^{null} (NOG) mice were obtained from the Central Institute for Experimental Animals (CIEA) and maintained in the animal facility of Tohoku University School of Medicine under specific pathogen-free conditions. NOG I-A$\beta^{-/-}$ mice or NOG I-A$\beta^{+/-}$ mice were obtained by backcrossing B6 I-A$\beta^{-/-}$ mice (26) kindly gifted from Mathis and Benoist (Harvard Medical School) onto the NOG background more than five times with a speed congenic technique (27) in CIEA. All the animal experiments were properly conducted according to the institutional guidelines. These mice were irradiated with 120 cGy of X-rays, and 1×10^5 cord blood $CD34^+$ cells, which were resuspended with 200 μl PBS, were transferred into them by intravenous (i.v.) injection later the same day.

Antibodies and flow cytometric analysis

The following mAbs were used. Anti-CD3–FITC, anti-CD4–FITC, anti-CD19–FITC, anti-CD34–FITC, anti-CD45–FITC, anti-CD62L–FITC, anti-CD69–FITC, anti-CD4–phycoerythrin (PE), anti-CD20–PE, anti-CD23–PE, anti-CD44–PE, anti-IgD–PE, anti-CD4–allophycocyanin (APC), anti-CD20–APC, anti-CD28–APC, anti-CD38–APC, ani-IgM–APC, anti-CD11b–APC, anti-CD8–PE–Cy7, anti-CD3–biotin, anti-IgD–biotin and anti-CD132–biotin were purchased from BD PharMingen (San Jose, CA, USA). Anti-CD24–FITC, anti-CD27–PE, anti-CD23–PE, anti-CD10–PE, anti-CD178–PE, anti-CD95–pacific blue, anti-CD19–APC Alexa Fluor 750 and e-Fluor 450 Mouse IgG1, k isotype control were from e-Bioscience (San Diego, CA, USA). Anti-CD5–PE-Cy7 and anti-CD24–PE-Cy5 were from Beckman Coulter (Miami, FL, USA). Anti-CD34–biotin was from Serotec. Anti-TRBV28 (Vβ3)–biotin was from Ancell (Bayport, MN, USA). Biotinylated antibodies were visualized by streptavidin–APC or streptavidin–PE-Cy7 (BD PharMingen). For intracellular staining, anti-human IgM–FITC was purchased from Dako (Glostrup, Denmark). PE-labeled anti-VpreB (HSL96) and $V_{\lambda 5}$ (HSL11) were kindly provided by Karasuyama (28).

To analyze human lymphocytes in the hu-HSC-NOG mice, multicolor cytometric analysis was performed using a FACS

Calibur or FACS Canto II (BD Biosciences). To monitor the reconstitution periodically, peripheral blood was taken from the retro-orbital venous plexus through heparinized pipettes. At the time of sacrifice, single-cell suspensions were prepared from the spleen or BM by mincing with metal mesh or by flushing the tibiae and femurs with PBS containing 2% FCS using a 27-gauge needle. The cells were stained with the relevant mAbs for 15 min on ice, then washed with cold PBS containing 2% FCS and stained with the appropriate secondary antibodies when necessary. We used Cytofix/Cytoperm solution (BD Biosciences) for intracellular staining, according to the manufacturer's instructions. After the final wash, the cells were subjected to flow cytometric analysis. The proportion of each lineage was calculated using CELL Quest or FACS Diva software (BD Biosciences).

ELISA

The concentration of human IgM and IgG in the sera of reconstituted NOG mice was measured using a human Ig assay kit (Bethyl, Denver, CO, USA). For the detection of keyhole limpet hemocyanin (KLH)-specific human IgM and IgG antibodies, humanized NOG mice were immunized two or three times once a week with an emulsion of 500 μg of KLH whole protein (Sigma, St Louis, MO, USA) with CFA (Difco Laboratories, Sparks, MD, USA) in total 100 μl by intra-peritoneal (i.p.) injection. The sera from the immunized mice were harvested 1 week after the final immunization. The specific antibodies against KLH were measured by a standard ELISA. Briefly, 96-well plates were coated with 10 μg ml^{-1} KLH at 4°C overnight. After washing and blocking with PBS containing 1% BSA, the collected serum samples were loaded. HRP-conjugated anti-human Ig antibody was used as a secondary antibody. Both anti-IgG-specific and anti-IgM-specific antibodies were purchased from Bethyl (Montgomery, TX, USA). *o*-Phenylenediamine was used as a substrate for detection. The absorbance at 450 nm was measured by a microplate reader. To detect peptide-specific Ig, we used a peptide-coating kit (Takara, Otsu, Japan), according to the instruction manual.

To detect cytokines in the supernatants, kits for IL-2, IFN-γ or IL-4 (BD Biosciences) were used according to the instruction manuals from the manufacturer.

In vitro cultures

The single-cell suspension of spleen cells from hu-HSC-NOG mice was prepared as described above 16–20 weeks after reconstitution. Human IgD^+ mature B cells were isolated by MACS LS column by using a biotin-conjugated anti-IgD mAb and anti-biotin microbeads. The purity of the isolated fraction was ~90%. The IgD^+ cells were cultured in RPMI medium supplemented with 10% FCS and antibiotics [penicillin G sodium (100 U ml^{-1}) and streptomycin sulfate (100 μg ml^{-1})]. The cells were stimulated with polyclonal anti-IgM antibody at 2 μg ml^{-1} (Jackson Immunoresearch, West Grove, PA. USA) or with *Staphylococcus aureus* cowan (SAC) at 0.01% (Calbiochem, Gibbstown, NJ, USA) in the presence or absence of 1 μg ml^{-1} anti-CD40 antibody (R&D, Minneapolis, MN, USA) with or without a mixture of 100 ng ml^{-1} IL-21 (Peprotech, Rocky Hill, NJ, USA) and 25 U ml^{-1} IL-2 (R&D) in a 96-well plate (2×10^5 in 200 μl per well) for 7 days. The IgM and IgG levels in the culture supernatants were determined by ELISA as described above.

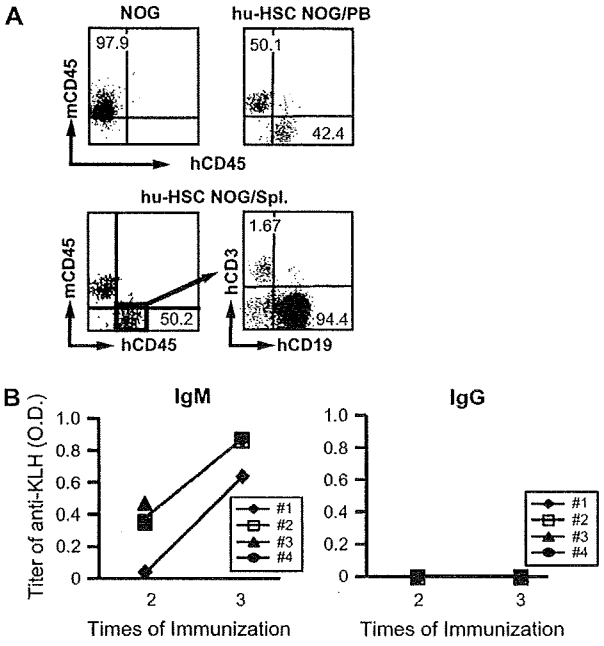

Fig. 1. Reconstitution of NOG mice with human hematopoietic stem cells. (A) Representative FACS analysis of peripheral blood (PB) cells from hu-HSC NOG mice 8 weeks after $CD34^+$ cell transplantation ($n = 6$). Engraftment of human $CD45^+$ ($hCD45^+$) cells in the PB in the hu-HSC NOG is shown (top left panel: control non-transferred NOG mouse, top right panel: hu-HSC NOG). Development of the human $CD19^+$ B cells and $CD3^+$ T cells in the spleen were analyzed in the hu-HSC NOG gated on $hCD45^+$ cells (bottom panels) (8 weeks after reconstitution, $n = 6$). (B) Humoral immune responses in hu-HSC NOG mice. Upon immunization of the hu-HSC NOG mice (at 16weeks after reconstitution, $n = 4$) with KLH/CFA emulsion (500 μg of KLH/CFA, three times), the sera was collected and examined for the presence of KLH-specific human IgM (left panel) or IgG (right panel) by ELISA.

For T-cell stimulation, the total spleen cells of hu-HSC NOG mice were cultured with PHA (1 μg ml^{-1}) or a mixture of soluble anti-CD3 (OKT3, 10 μg ml^{-1}) (BD PharMingen) and anti-CD28 (1 μg ml^{-1}) (Biolegend, San Diego, CA, USA) antibodies in a 96-well round-bottom plate (1×10^5 in 200 μl per well). Human $CD4^+$ or $CD8^+$ T cells in the hu-HSC NOG mice were purified by positive selection by MACS LS column in combination with anti-human CD4 or CD8 microbeads, respectively. The T cells were stimulated with immobilized anti-CD3 (10 μg ml^{-1}) and CD28 (1 μg ml^{-1}) antibodies or mixture of phorbol myristate acetate (50 ng ml^{-1}) and ionomycin (1 μg ml^{-1}) in 96-well round-bottom plates (1×10^5 in 200 μl per well). The T-cell proliferation was measured as the incorporation of [^{3}H]thymidine for the last 6 h of a 72-h culture. Carboxyfluorescein succinimidyl ester (CFSE) labeling was conducted according to a standard protocol.

Reverse transcription–PCR

The expression of mRNA for AID was measured by semi-quantitative reverse transcription (RT)–PCR. The total RNA

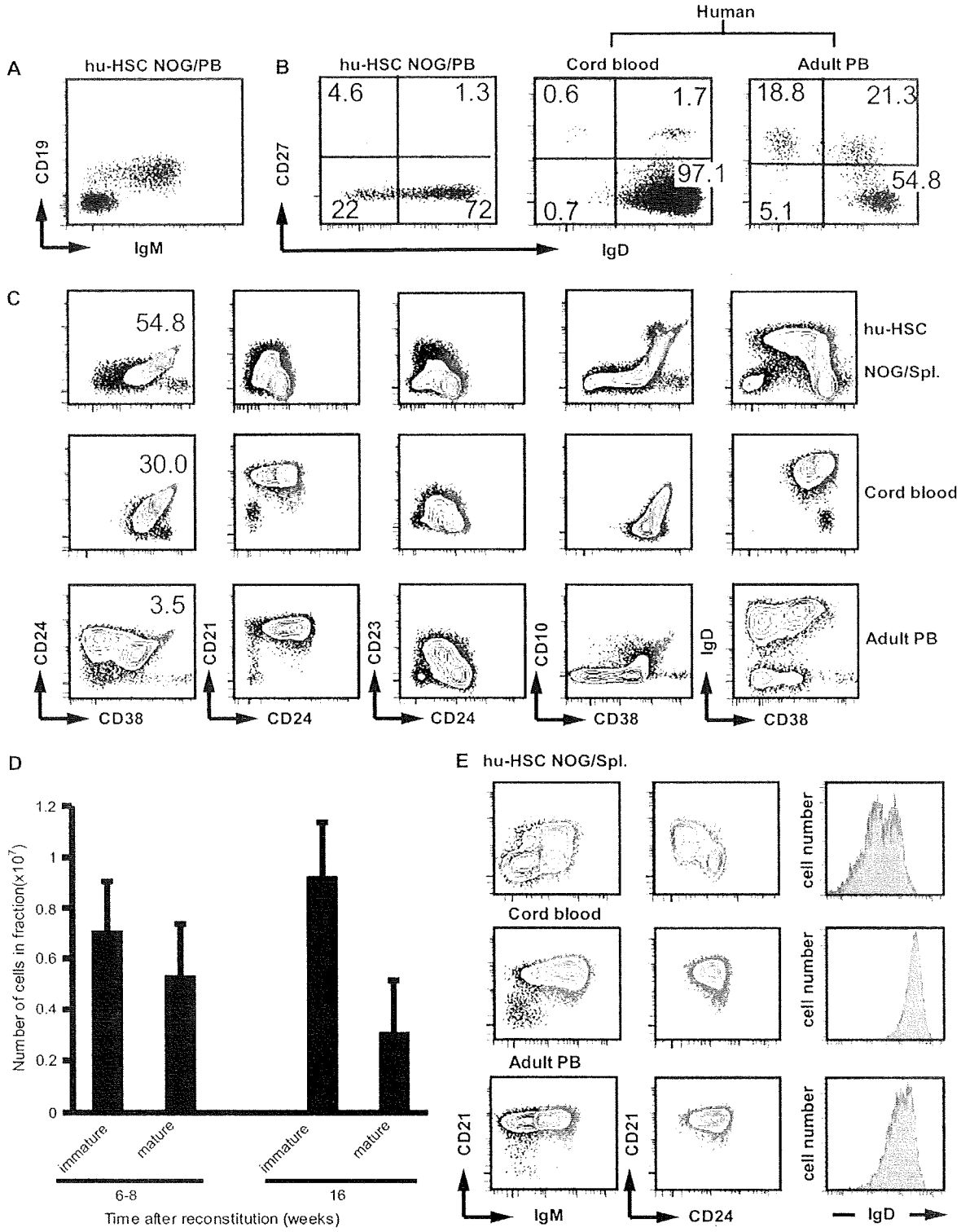

Fig. 2. Analysis of B cells in hu-HSC NOG. (A) Characterization of human B cells in the peripheral blood (PB) of hu-HSC NOG. A representative result of staining with anti-IgM and anti-CD19 antibodies was shown (16 weeks after reconstitution, $n = 6$). (B) Representative staining patterns with anti-IgD and anti-CD27 antibodies are shown gated on $CD19^+$ B cells from various sources [i.e. PB of the hu-HSC NOG (16 weeks after reconstitution, $n = 3$), human cord blood or PB of a normal healthy adult]. (C) A representative analysis of splenic $CD19^+$ cells in hu-HSC NOG by various differentiation-related markers. The whole-spleen cells of the hu-HSC NOG mice (8 weeks after reconstitution, $n = 4$), cord blood-derived

was prepared from cells using Trizol Reagent (Invitrogen, Carlsbad, CA, USA). The concentration of the total RNA was measured by NanoDrop 1000 (Nanodrop Technologies), and the first-strand cDNA was synthesized using SuperscriptIII (Invitrogen) with an oligo (dT) 20 primer. The cDNA for AID, RAG1, RAG2, TdT or glyceraldehyde 3-phosphate dehydrogenase (GAPDH) was amplified with specific primers using Ex-Taq polymerase (Takara). The primer sets were as follows—AID: forward, 5′-gaggcaagaagacactctgg and reverse, 5′–caaaaggatgcgccgaagctgtctggag; RAG1: forward, 5′-ccagctgtttgcttggccatccgt and reverse, 5′-ttgggatctcatgccttccaagat; RAG2: forward, 5′-atgtccctgcagatggtaaca and reverse, 5′-gcctttgtatgagcaagtagc; TdT: forward, 5′-ccaccaattgctgtacaaaaga and reverse, 5′-tcgttcatcatttaacacagctt; β-actin: forward, 5′-gctcgtcgtcgacaacggctc and reverse, 5′-caaacatgatctgggtcatcttctc and GAPDH: forward, 5′-gaaggtgaaggtcggagtca and reverse, 5′-ttcacacccatgacgaacat.

After denaturing at 94°C for 5 min, the cDNA was amplified by a protocol consisting of 94°C for 30 s, 60°C for 30 s and 72°C for 30 s, for 25 cycles. The PCR products were separated on agarose gels and stained with ethidium bromide.

Retroviral vectors

The retroviral vector, pDΔNsam-IRES-EGFP, based on murine stem cell virus with enhanced green fluorescent protein (EGFP) as a marker under an internal ribosomal entry site (IRES) was kindly provided by Onodera (29). PLAT-F, a package cell line that produces a pseudotype virus with an RD114 envelope, was from Kitamura (30) and used to infect $CD34^+$ stem cells. The human *bcl-2* or *HLA-DRB*0401* genes were inserted into the *Not*I and *Bam*HI sites of the pDΔNsam-IRES-EGFP vector.

B16 T cells specific for an influenza hemagglutinin peptide ($HA_{307-319}$) were kindly provided by Buckner (31). The T-cell receptor (TCR) genes (B16 TCR; *TRAV4* and *TRBV28* based on the International Immunogenetics Information System) were isolated by standard techniques from the B16 T cells and cloned into the retroviral vector. *TRAV4* was inserted into the *Not*I/*Bam*HI sites, while *TRBV28* was inserted into the *Nco*I/*Cla*I sites after removing the EGFP gene. To infect human T cells, retrovirus was prepared in the form of a VSV-pseudotype virus in 293T packaging cells, by plasmid DNA transfection using a standard calcium phosphate protocol. After 72 h, the supernatants were recovered and concentrated by centrifugation at 8700 r.p.m. for 19 h at 4°C.

Gene delivery into $CD34^+$ cells by retrovirus

$CD34^+$ cells isolated from cord blood were cultured in X-VIVO 15 (Cambrex Bioscience, Walkersville, MD, USA), supplemented with 1% human serum albumin (HSA) (Kaketsuken, Kumamoto, Japan) and stimulated with a cytokine cocktail [100 ng ml^{-1} stem cell factor (R&D), 100 ng ml^{-1} Flt-3 ligand (Flt-3L) (R&D), 100 ng ml^{-1} thrombopoietin and 100 ng ml^{-1} IL-6 (Peprotech)] in a 24-well plate (2×10^5 per well) for 48 h. During the priming of the $CD34^+$ cells, non-tissue culture-treated six-well plates (Becton Dickinson) were coated with CH-296 recombinant fibronectin fragment (Retronectin) (20 μg ml^{-1}, Takara). The stimulated $CD34^+$ cells were harvested and placed in the CH-296-coated plates (3×10^5 per well) in the presence of the respective virus supernatant. The supernatants were diluted 1:2 with X-VIVO containing 1% HSA, 10 μg ml^{-1} protamine sulfate and the cytokine mixture described above. The cells were spun at 2000 r.p.m. for 30 min at 37°C. Every 12 h, the medium was replaced with fresh virus supernatant. After 48 h of culture, the frequency of GFP- and CD34-expressing cells was examined. About 5×10^5 to 1×10^6 infected cells were injected i.v. into irradiated NOG mice.

Retroviral infection of human T cells

$CD4^+$ T cells were isolated from the PBMCs of normal healthy donors by MACS, as described above. The infection of T cells by retrovirus for B16 TCR was conducted as previously reported (32). Briefly, purified T cells were stimulated in the presence of recombinant human IL-2 (50 U ml^{-1}) on a 24-well plate that had been previously coated with anti-CD3 antibody (1 μg ml^{-1}), anti-CD28 antibody (1 μg ml^{-1}) and Retronectin (12 μg ml^{-1}). Half of the culture medium was replaced by fresh medium supplemented with IL-2 every 48 h. On days 4 and 5, the T cells were spin-infected with the concentrated virus (2000 r.p.m., 90 min at 32°C). After a further 1 week of culture, the expression of B16 TCR on the T cells was examined by staining with anti-TRBV28 antibody, APC-conjugated HLA-DRB1*0401/$HA_{307-319}$ (PKYVKQNTLKLAT) or HLA-DRB1*0401/human $CLIP_{103-117}$ (PVSKMRMATPLLMQA) tetramers (kindly provided by National Institute of Health tetramer core facility). These T cells (1×10^6 or 3×10^6) were transferred into reconstituted NOG mice by i.v. injection and subsequently i.p. immunized with HA peptide/CFA emulsion (100 μg HA peptide in total 100 μl).

Results

Reconstitution of NOG mice with human $CD34^+$ stem cells

In the fully reconstituted NOG mice, a significant amount of human B and T cells appeared in the peripheral blood and comprised major fractions in the spleen, as previously reported (16) (Fig. 1A). Immunization of the hu-HSC NOG mice with a protein antigen, KLH, with CFA evoked an antigen-specific IgM response, but a negligible antigen-specific IgG response (Fig. 1B). This finding was also consistent with previous reports (21, 22, 24, 25).

Analysis of the human B cells in hu-HSC NOG mice: partial differentiation of the human B cells

To elucidate the mechanisms for the poor IgG response in the hu-HSC NOG mice, we analyzed the development and

cells or PB from a normal adult were stained with respective antibodies. $CD24^{int/hi}CD38^{hi}$ immature population is highlighted by red contour plot. (D) The number of immature ($CD19^+CD24^{int/hi}CD38^{hi}$) or mature ($CD19^+CD24^{lo}CD38^{lo}$) B cells from hu-HSC NOG at different time points after reconstitution. The means of the cell number of each B-cell population are represented with standard deviation ($n = 3$ for each group). (E) Partial differentiation of human B cells in the spleen in hu-HSC NOG mice. The expression patterns of CD24, CD21 or IgD on $CD19^+IgM^+$ B cells (highlighted by blue contour plot) from the hu-HSC NOG mice (8 weeks after reconstitution, $n = 4$), cord blood or adult PB are shown.

differentiation of the human B cells in these mice in detail. Most of the human B cells in the peripheral blood of the hu-HSC NOG mice were IgM and/or IgD positive (Fig. 2A). Few $CD27^+$ B cells were detected, indicating that almost all the B cells were in a naive state (Fig. 2B). This phenotype was different from that of the human B cells in PBMCs obtained from normal healthy donors or cord blood, which clearly consisted of three major subsets: $IgM^+IgD^+CD27^-$-naive B cells, $IgM^+IgD^+CD27^+$-activated or non-switched memory B cells and IgD^-CD27^+ memory B cells (Fig. 2B).

The analysis of the human B cells in the spleen from the hu-HSC NOG mice for two developmentally regulated markers, CD24 and CD38, revealed an unusual accumulation of $CD24^{int/hi}CD38^{hi}$ immature B cells in the spleen (Fig. 2C). This $CD24^{int/hi}CD38^{hi}$ population comprised up to 60% (62.0 ± 13.8%, $n = 6$) of the splenic $CD19^+$ cells on average in the hu-HSC NOG mice. The frequency was lower at early time points after reconstitution but gradually increased; i.e. ~50% (53.3 ± 8.0%, $n = 3$) 6–8 weeks after reconstitution and ~70% (70.7 ± 13.7%, $n = 3$) 16 weeks after (Fig. 2D). Although a similar $CD24^{int/hi}CD38^{hi}$ population was also evident in the cord blood B cells or PBMCs (~30% or 2–3% in $CD19^+$ cells, respectively) (Fig. 2C), the $CD24^{int/hi}CD38^{hi}$ population in the hu-HSC NOG mice showed an even more immature phenotype (Fig. 2C); i.e. the former was $CD21^{hi}$ $CD23^{int}CD10^{lo}$ IgD^{hi}, while the latter was $CD21^-CD23^-CD10^{int/hi}IgD^{-/lo}$. Besides the $CD24^{int/hi}CD38^{hi}$ population, even when gated on more mature IgM^+ B cells, ~25% of the cells in the hu-HSC NOG mice were still $CD24^{hi}CD21^-IgD^{-/lo}$ (Fig. 2E), resembling the phenotype of transitional type 1 (T1) B cells (33). These analyses collectively suggested that the human B cells were only partially differentiated in the hu-HSC NOG mice.

Accumulation of B-cell precursors in the spleen of hu-HSC NOG mice

We also noticed the presence of a large number of $CD19^+CD24^{int/hi}CD38^{hi}IgM^-IgD^-$ cells (~40% of the $CD19^+$ population) in the spleen of the hu-HSC NOG mice (Fig. 3A, left panel). Because of their immature phenotype, we suspected these cells to be B-cell progenitors. Further dissection of the $CD19^+IgM^-IgD^-$ population using anti-CD20 and CD34 antibodies demonstrated that they consisted of at least three fractions: $CD20^-CD34^+$, $CD20^-CD34^-$ and $CD20^+CD34^-$ B cells (Fig. 3A, right panel). Since B cells with these phenotypes are known to comprise immature B-cell lineages in the BM, we examined the BM cells in the hu-HSC NOG mice. As expected, $CD19^+IgM^-CD20^-CD34^+$ pro-B and $CD19^+IgM^-CD20^-CD34^-$ pre-B cells were detected (Fig. 3B). The expression of CD179 (V_{preB}) and cytoplasmic μ chain (cμ) was also examined by intracellular staining. There were three distinct populations with different expression patterns for CD179 and cμ: $CD179^+c\mu^-$ pro-B, $CD179^+c\mu^+$ pre-B and $CD179^-c\mu^+$ populations, both in the spleen and BM (Fig. 3C and D). We obtained similar results for $V_{\lambda 5}$ (data not shown). RT–PCR analyses showed that the pro-B- or pre-B-like cells in the spleen expressed RAG and TdT, with patterns similar to those of the pro-B and pre-B cells in the BM (Fig. 3E).

In addition to the presence of phenotypically pro-B- and pre-B-like cells in the spleen of the hu-HSC NOG mice, further immature B-cell lineages, i.e. early-B cells or common lymphoid progenitors, were detected in the spleen. Using CD38 and CD10 (34, 35), a clear $CD19^-CD38^+CD10^+CD34^+$ early-B-cell population was detected in the spleen as well as in the BM (Fig. 3F and G). These results collectively suggest that early precursors in the B-cell lineage were present in the spleen of the humanized NOG mice.

IgG response of the human B cells from hu-HSC NOG mice to in vitro stimulation

The poor production of IgG in the hu-HSC NOG mice might have been attributed to the inappropriate differentiation of human B cells in the mouse environment. To examine the intrinsic capability of the B cells for the IgG response, we used an *in vitro* culture system. IgD^+CD19^+-naive mature B cells were purified from the spleen of hu-HSC NOG mice and stimulated with SAC as quasi-antigens in the presence or absence of anti-CD40 antibody. IL-21/IL-2 was also provided because these cytokines, especially IL-21, are potent inducers of naive B-cell differentiation into antibody-secreting cells *in vitro* (36, 37). Significant amounts of both IgM and IgG were detected in the supernatants after a 7-day culture (Fig. 4A). The IgG level was comparable to that of normal B cells from healthy donors (data not shown). Antigenic stimulation together with IL2/IL-21 also induced the formation of IgD^-CD38^+ antibody-secreting cells (Fig. 4B). In addition, IgD^-CD27^+ cells appeared toward the end of the culture period (Fig. 4B). The antibody class switch in these B cells was further supported by the induction of AID mRNA in the cultured B cells (Fig. 4C). These results suggested that the human B cells with a mature phenotype in hu-HSC NOG mice could respond to antigenic stimulation and had the functional molecular machinery for the Ig class switch.

Analysis of the human T cells in hu-HSC NOG mice: impaired function of $CD4^+$ T cells

Since the human B cells from hu-HSC NOG mice could produce IgG *in vitro*, we next examined the T cells in the hu-HSC NOG mice. The development of human $CD4^+$ and $CD8^+$ T cells was detected in the thymus and spleen of the hu-HSC NOG mice (Fig. 5A). Initially, we compared the expression patterns of several T-cell-related antigens and cytokine receptors: CD28, CD44, CD62L, CD132 (γc) and IL-7Rα chain (Fig. 5B). There were, however, no significant differences in these molecules between the T cells from the hu-HSC NOG mice and PBMCs.

To address the functionality of the T cells, we stimulated the whole-spleen cells from hu-HSC NOG mice with PHA or a mixture of soluble anti-CD3 and anti-CD28 antibodies in *in vitro* culture systems. The hu-HSC NOG spleen cells showed significant proliferation after 3 days in culture, consistent with previous reports (Fig. 5C). However, when the whole-spleen cells from the hu-HSC NOG mice previously immunized with KLH were re-stimulated in the presence of KLH *in vitro*, we could hardly detect IFN-γ and IL-4 (data not shown). This result was in agreement with the poor IgG production in the hu-HSC NOG mice.

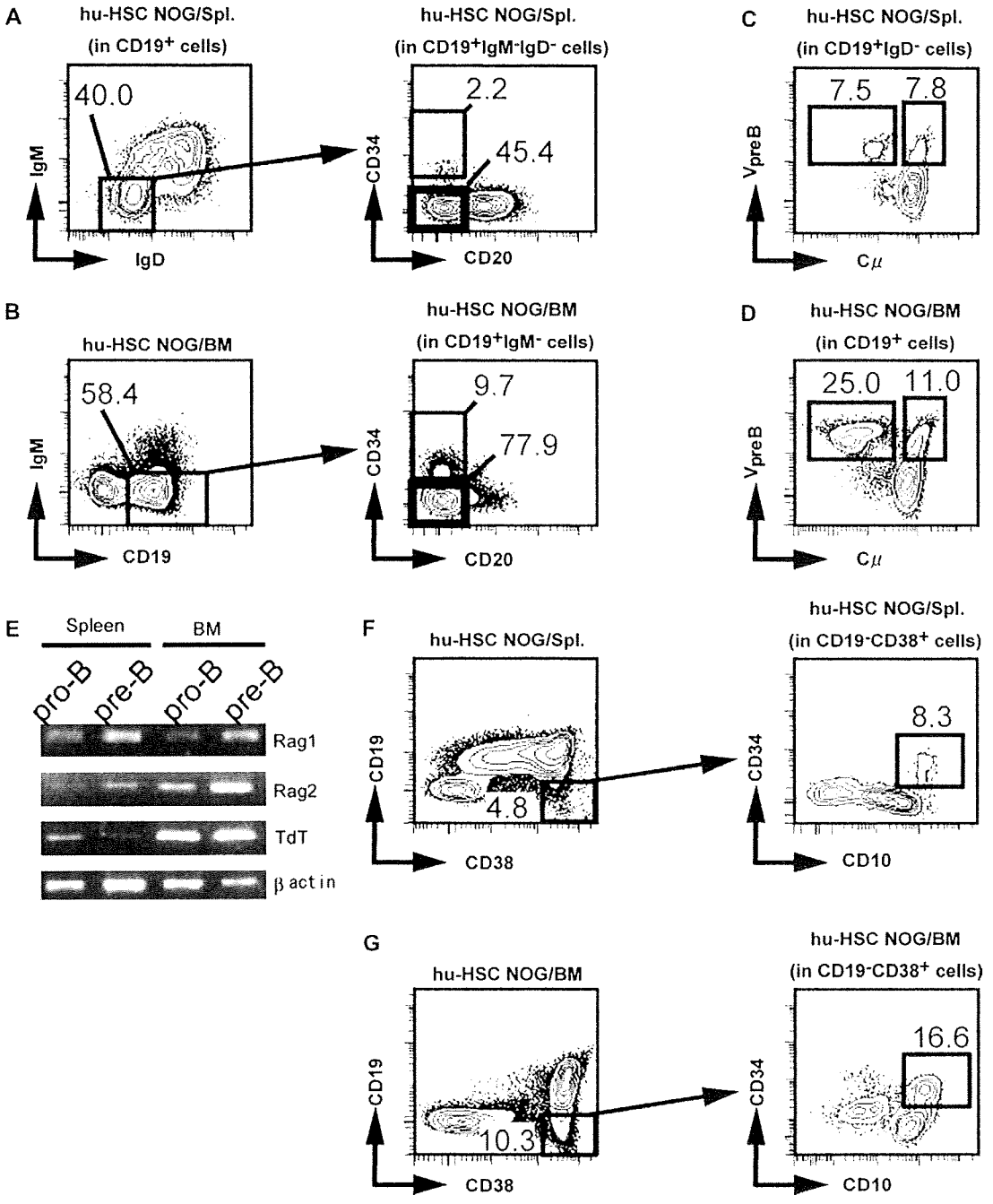

Fig. 3. Accumulation of human B-cell progenitors in the spleen of hu-HSC NOG mice. (A and B) Representative staining data of spleen (A) or BM (B) of hu-HSC NOG mice. The spleen cells or BM from hu-HSC NOG mice (8 weeks after reconstitution, $n = 4$) were stained with anti-CD19, anti-IgM and anti-IgD antibodies as described in Methods (left panels). The $CD19^+IgD^-$ IgM^- or $CD19^+IgM^+$ cells (represented by rectangles) in the spleen or BM, respectively, were further analyzed for the expression of CD34 and CD20. $CD34^+CD20^-$ (gated by thin rectangle) or $CD34^-CD20^+$ B cells (gated by bold rectangle) represent pro-B or pre-B cells, respectively. (C and D) Expression of V_{preB} in B cells in hu-HSC NOG mice. $CD19^+IgD^-$ cells in the spleen (C) or $CD19^+$ cells in BM (D) were examined for V_{preB} with cμ by intracellular staining (8 weeks after reconstitution, $n = 3$). The gated $V_{preB}^+c\mu^-$ or $V_{preB}^+c\mu^+$ cells represent pro-B cells or pre-B cells, respectively. (E) Analyses of gene expression in human B-cell progenitors in hu-HSC NOG mice. cDNA was prepared from $CD19^+IgM^-$ $CD34^+$ $CD10^+$ pre-B or $CD19^+IgM^-$ $CD34^+CD10^+$ pro-B cells in the spleen or BM of the hu-HSC NOG mice (8 weeks after reconstitution). The expression of RAG-1, RAG-2 or TdT was examined by semi-quantitative RT-PCR as described in Methods. A representative result of three independent experiments is shown. (F and G) Detection of early-B cells in the spleen (F) or BM (G) in hu-HSC NOG mice. Cells were stained with anti-CD19 and anti-CD38 antibodies (left panels). The expression of CD10 and CD34 in $CD19^+$ $CD38^+$ gated cells were further examined (8 weeks after reconstitution, $n = 3$). The gated $CD19^+$ $CD38^+CD10^+CD34^+$ cells represent early-B or common lymphoid progenitors cells.

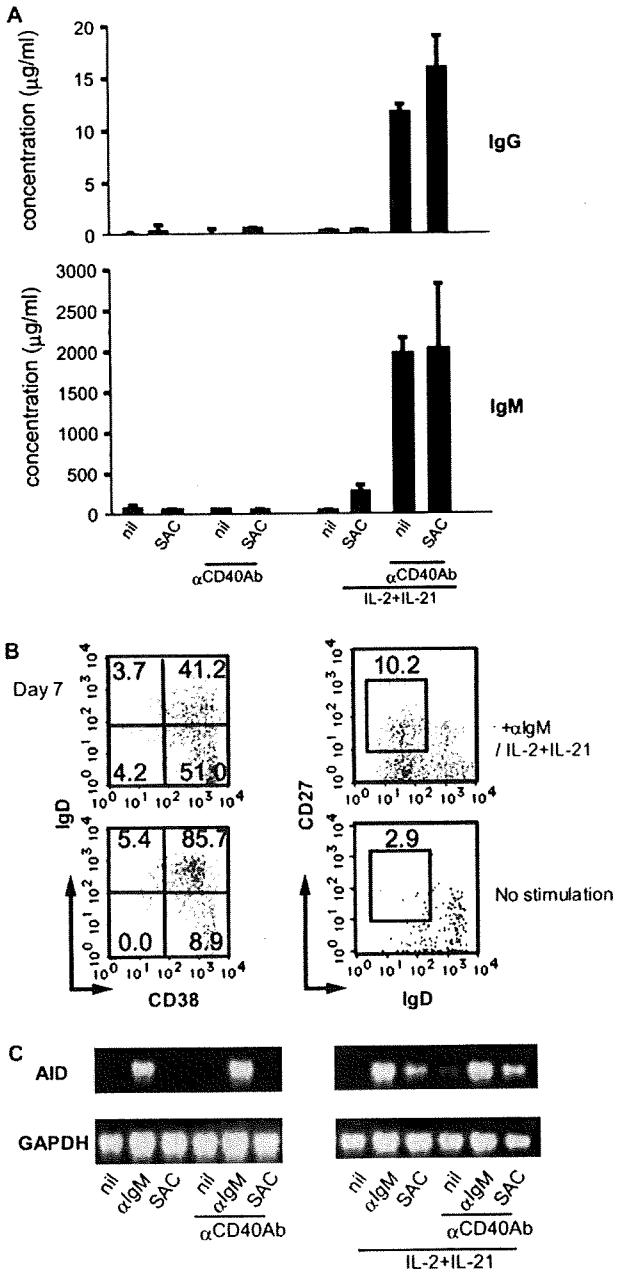

Fig. 4. Analysis of immune response of human B cells in hu-HSC NOG mice *in vitro*. (A) Purified IgD$^+$ splenic B cells in the hu-HSC NOG mice (8–16 weeks after reconstitution, $n = 4$) were stimulated *in vitro* with SAC (0.01%), in the presence or absence of anti-CD40 polyclonal antibody (1 μg ml^{-1}), with or without IL-2 (25 U ml^{-1})/IL-21 (100 ng ml^{-1}); secretion of IgM and IgG by 7-day cultured human B cells. Each culture supernatant was harvested and the amounts of human IgM (lower panal) and IgG (upper panel) were quantified by ELISA as described in Methods. (B) Analysis of surface antigen expression on CD19$^+$ splenic B cells in hu-HSC NOG mice (8–16 weeks after reconstitution) after *in vitro* stimulation with or without polyclonal anti-IgM antibody and cytokines. After 1-week culture, the B cells were recovered and stained with anti-CD38, anti-CD27 and anti-IgD antibodies. A representative result of three independent cultures is shown. (C) Total RNA was extracted from the B cells 3 days after *in vitro* culture with various stimulations, followed by synthesis of cDNA. The expression of AID or GAPDH was investigated by RT–PCR. A representative result of three independent cultures is shown.

Although we observed the activation of the spleen cells of the hu-HSC NOG mice, the magnitude was quite low compared with that of the cultured PBMCs. To exclude the contributions of antigen-presenting cells and analyze the T cells directly, we used purified CD4$^+$ and CD8$^+$ T cells. When the purified T cells were stimulated with immobilized anti-CD3 and anti-CD28 antibodies, they showed significant proliferation compared with the culture without stimulation. However, the intensity of their response, especially that of the CD4$^+$ T cells, was markedly lower than that of normal T cells isolated from PBMCs (Fig. 6A, left panel). The cumulative data showed that the magnitude of the proliferation of CD4$^+$ T cells from the hu-HSC NOG mice was no more than 10% of the normal CD4$^+$ T-cell response (Fig. 6A, right panel). For the CD8$^+$ T cells, the tendency was less clear because there was a large variance among mice (Fig. 6A). The T cells from the hu-HSC NOG mice also showed only modest proliferation even when they were strongly stimulated with PMA and ionomycin (Fig. 6B). The amount of IL-2 produced by the cultured T cells was remarkably low, consistent with their low proliferation (Fig. 6C). Addition of exogenous IL-2 (100 IU ml^{-1}) did not restore the proliferation of the human T cells from the hu-HSC NOG mice (data not shown).

Mechanisms of the impaired response of the human T cells in hu-HSC NOG mice

To examine the mechanisms of the hyporesponse of the T cells in the hu-HSC NOG mice, we analyzed the expression of CD25 and CD69 after stimulation. These molecules were detected on both CD4$^+$ and CD8$^+$ T cells, at similar levels as on normal T cells from PBMCs (Fig. 7A). When the number of viable cells was enumerated, however, there were significant differences between the hu-HSC NOG T cells and PBMC T cells. AnnexinV and propidium iodide (PI) staining of cultured T cells demonstrated that >50% of the CD4$^+$ T cells from hu-HSC NOG mice were dead at 24 h, while only 10% of the PBMC T cells were (Fig. 7B). At 48 h, nearly 80% of the CD4$^+$ T cells from hu-HSC NOG mice were PI positive. The CD8$^+$ T cells showed different patterns among mice. In the half of the animals, nearly 80% of the CD8$^+$ T cells died after a 24-h culture, while in the remaining half, 60% of the cells were still alive after a 72-h culture (Fig. 7C). To investigate the higher susceptibility of the T cells in the hu-HSC NOG mice to cell death, we examined the expression of CD95 (Fas) and CD178 (FasL) on the T cells. A significant expression of CD95 (Fig. 7D) but not CD178 (data not shown) was detected on the T cells from the hu-HSC NOG mice. In the human T cells from PBMCs, there were two populations, CD95$^+$ and CD95$^-$, while in the hu-HSC NOG mice, most of the T cells expressed similar amounts of CD95 on their surface (Fig. 7D).

We next addressed whether the impairment of T-cell functions was already conferred to the T cells in the thymus of the hu-HSC NOG mice. CD4$^+$CD8$^-$ single-positive (SP) thymocytes were prepared from the hu-HSC NOG mice. Because the number of thymocytes in a hu-HSC NOG mouse was usually not sufficient for analysis, we introduced the *bcl-2* gene into the CD34$^+$ stem cells by retrovirus *in vitro* before transplantation in an effort to increase the cell number. Indeed, in such hu-HSC (*bcl-2*) NOG mice, the

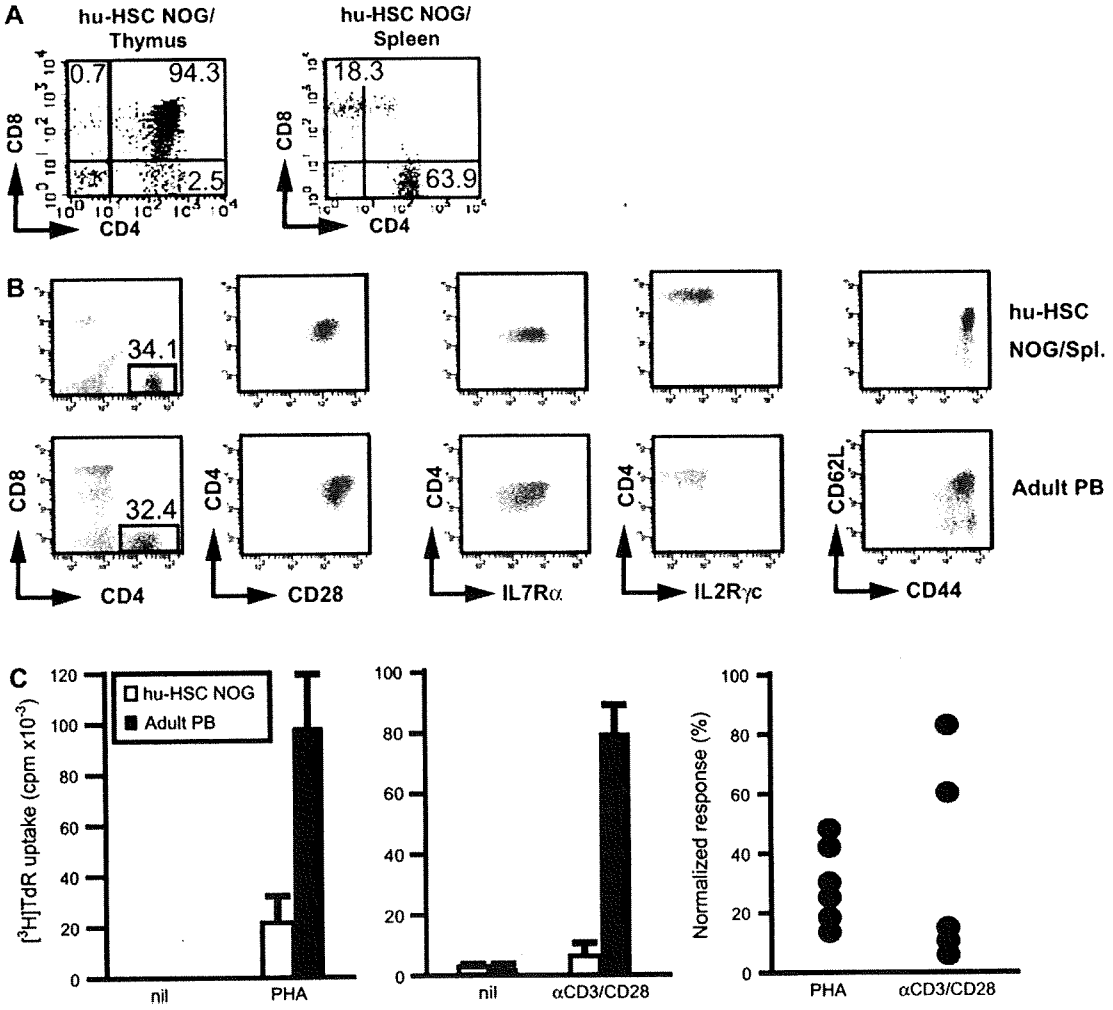

Fig. 5. Analysis of human T cells developed in hu-HSC NOG mice. (A) Development of human T cells in the thymus and spleen in hu-HSC NOG mice. Single-cell suspensions from each organ were stained with anti-CD4 and anti-CD8 antibodies (20 weeks after reconstitution, $n = 4$). (B) A representative staining for various molecules on human T cells from hu-HSC NOG mice. Whole-spleen cells from the hu-HSC NOG mice (20 weeks after reconstitution, $n = 3$) or adult peripheral blood (PB) were stained with indicated antibodies. $CD4^+$ T-cell population (gated by rectangles and highlighted by red dot plots) was further examined for each molecule. (C) Analysis of functions of human T cells in hu-HSC NOG mice *in vitro*. Whole splenocytes from the hu-HSC NOG mice (20 weeks after reconstitution) (white bar) or normal adult PB (black bar) were stimulated with PHA (left panel, $n = 6$) or mixture of soluble anti-CD3 and anti-CD28 antibodies (middle panel, $n = 5$). After 72-h culture, the proliferation of T cells was measured as the amounts of incorporated [^{3}H]thymidine ([^{3}H]TdR). Representative data are shown. The means from triplicated cultures are shown. The cumulative data are shown after normalizing the magnitude of the response of hu-HSC NOG T cells to that of PB T cells (right panel).

exogenous Bcl-2 was expressed at a high level (Fig. 8A), and the effect on increasing the thymocytes was remarkable (no more than 1×10^6 in each mouse with control GFP vector versus $\sim 6 \times 10^6$ in *bcl-2* group), although the differentiation of B or T cells in the spleen was not affected (data not shown). We isolated the $CD4^+CD8^-$ SP thymocytes or splenic $CD4^+$ T cells from the hu-HSC (*bcl-2*) NOG mice and stimulated them as described above. The $CD4^+CD8^-$ SP cells showed vigorous proliferation, as high as that of normal T cells from PBMCs (Fig. 8B). A significant amount of IL-2 was also detected in the culture supernatants of the $CD4^+CD8^-$ SP cells (Fig. 8C). Interestingly, the splenic $CD4^+$ T cells from the same mice did not show proliferation (Fig. 8B). Consistently, immunization of the hu-HSC (*bcl-2*) NOG mice did not evoke an immune response in spite of the improvement in cell number (data not shown). Thus, the unresponsiveness of the T cells in the hu-HSC NOG mice was induced in the periphery, not in the thymus. Notably, the $CD4^+$ T cells from the hu-HSC (*bcl-2*) NOG mice showed better viability compared with the $CD4^+$ T cells from the usual hu-HSC NOG mice; 60–80% of the cultured cells were still viable after 48 h (data not shown). Hence, the poor response of the T cells from hu-HSC NOG mice was not solely due to their high susceptibility to cell death, but other mechanisms (such as induction of anergy) were also involved.

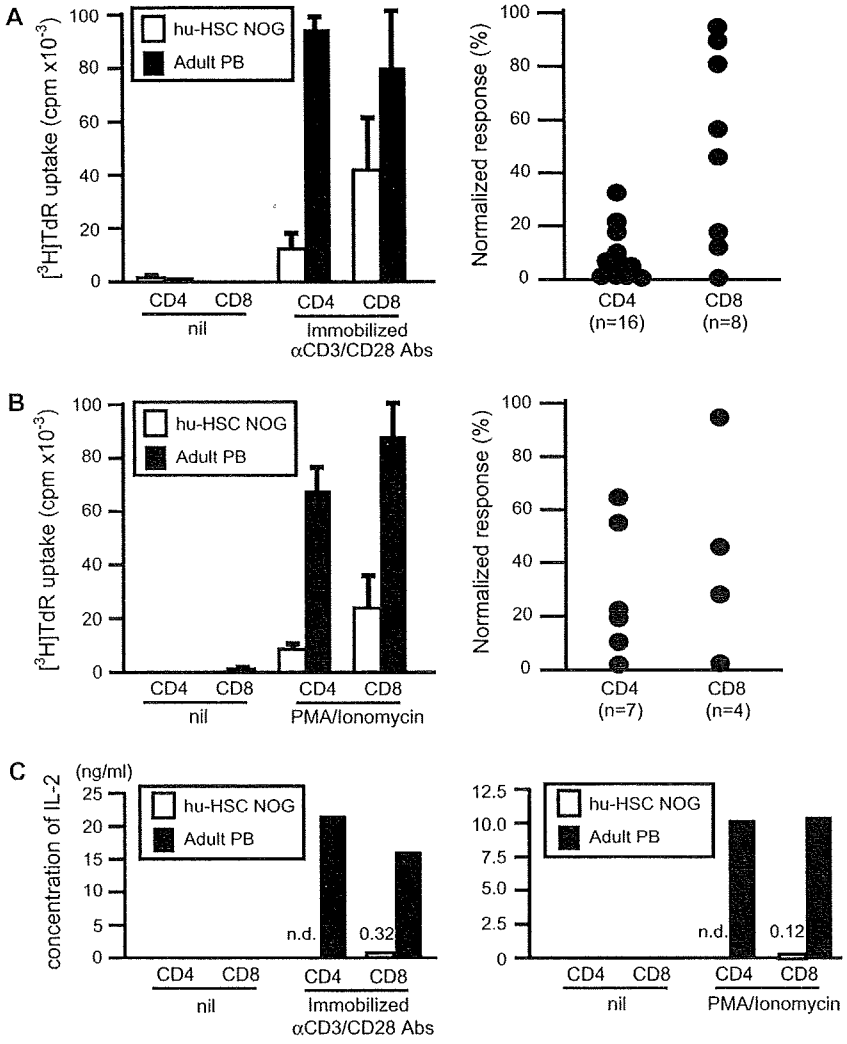

Fig. 6. Impaired responses of human T cells in hu-HSC NOG mice to mitogens. (A and B) Analysis of functions of human $CD4^+$ or $CD8^+$ T cells in hu-HSC NOG mice *in vitro*. $CD4^+$ or $CD8^+$ T cells were prepared from the spleen of the hu-HSC NOG mice (20 weeks after reconstitution) (white bar) or normal adult peripheral blood (PB) (black bar) as described in Methods. They were stimulated with immobilized anti-CD3 and anti-CD28 antibodies (A, left panel, $n = 16$ or 8 for $CD4^+$ T cells or $CD8^+$ T cells, respectively) or combination of PMA and ionomycin (B, left panel, $n = 7$ or 4 for $CD4^+$ T cells or $CD8^+$ T cells, respectively). After 72-h culture, the proliferation of T cells was measured as the amounts of incorporated [^{3}H]thymidine ([^{3}H]TdR) as in Fig. 5(C). The cumulative data are shown after normalizing the magnitude of the response of hu-HSC NOG T cells to that of PB T cells (right panels). (C) Quantification of IL-2 produced by human T cells in hu-HSC NOG mice *in vitro*. The amount of IL-2 in the supernatants obtained from the *in vitro* cultures described in (A and B) was measured by ELISA. n.d.: under detection level by ELISA.

Development of human T cells in NOG I-Aβ$^{-/-}$ mice

The results with the $CD4^+CD8^-$ SP thymocytes suggested that there were regulatory mechanisms to induce tolerance to the human T cells in the mouse periphery. To examine the involvement of mouse MHC molecules, we used the NOG I-Aβ$^{-/-}$ strain. In these mice, we could not detect any mouse $CD4^+$ T cells, as previously reported. Upon humanization, surprisingly, human T cells could be detected in the spleen of the hu-HSC NOG I-Aβ$^{-/-}$ mice (Fig. 9A). Thus, the HLA class II molecules on the human T cells (38) or a quite small number of human B cells or human dendritic cells (DCs) in the thymus positively selected human T cells in the mouse thymus. Although we could not detect a significant number of $CD4^+CD8^-$ SP thymocytes in the hu-HSC NOG I-Aβ$^{-/-}$ mice by FACS analysis after 20 weeks of reconstitution (Fig. 9B), these $CD4^+$ T cells were not derived from extrathymic tissues because no human T cells appeared in hu-HSC NOG *nu/nu* mice (data not shown), suggesting that the mouse thymus was indispensable for the human T-cell development. The number of $CD4^+$ T cells in the spleen was <1% of that in the regular hu-HSC NOG mice at 16 weeks after reconstitution and reached 20% at ~20 weeks (4.9×10^5, $n = 15$, in the regular hu-HSC NOG versus 1.2×10^5, $n = 4$, in the hu-HSC NOG I-Aβ$^{-/-}$ NOG). It is uncertain whether this increase was caused by the homeostatic proliferation

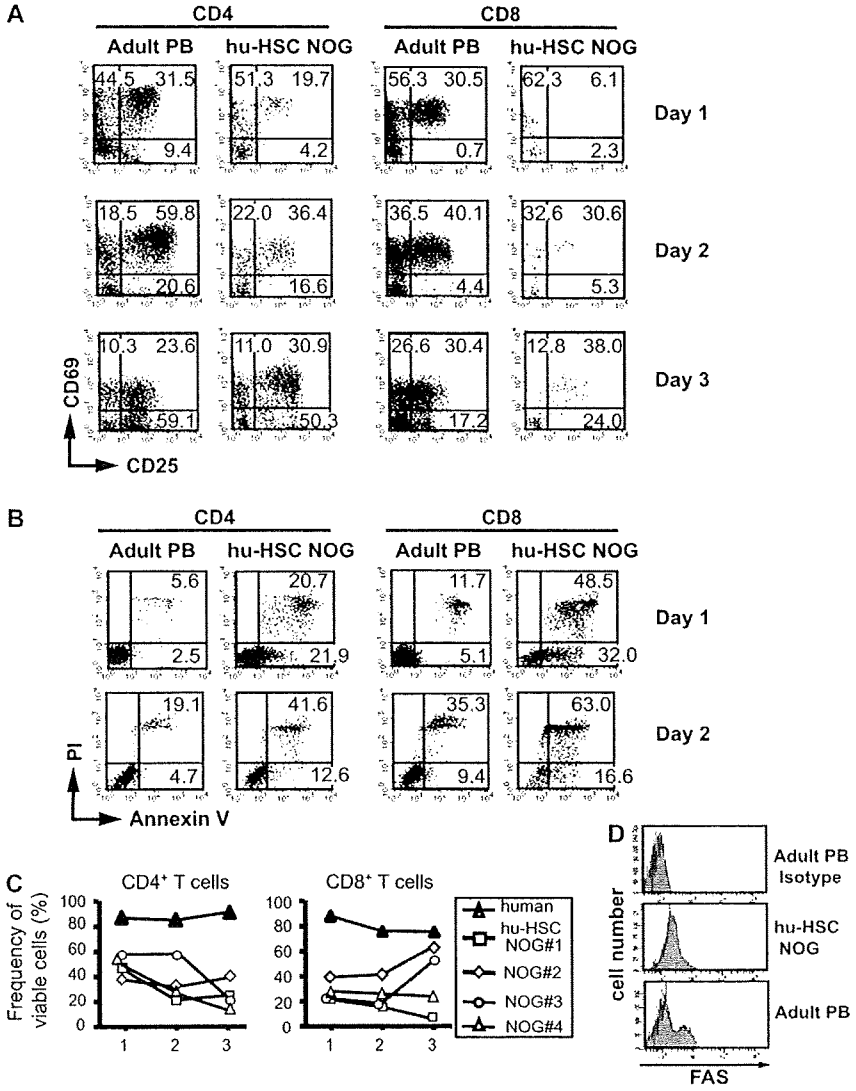

Fig. 7. Enhanced cell death of hu-HSC NOG T cells. (A) Analysis of activation markers of T cells. Purified $CD4^+$ or $CD8^+$ T cells from hu-HSC NOG mice (20 weeks after reconstitution) or human peripheral blood (PB) were stimulated by immobilized anti-CD3 and anti-CD28 antibodies as described in Fig. 6. The expression of CD25 and CD69 on them were analyzed every 24 h. A representative result from three independent animals is shown. (B) Analysis of apoptosis induced in T cells. The *in vitro* cultured $CD4^+$ or $CD8^+$ T cells as in (A) were stained with annexin V and PI at 24 and 48 h. A representative result from four independent experiments is shown. (C) Survival curve of *in vitro* cultured T cells. The frequency of viable $CD4^+$ or $CD8^+$ T cells was represented as the percentage of annexin V and PI double-negative cells in the FACS analysis mentioned in (B). (D) Expression analysis of CD95 (Fas) on T cells. A representative result of staining with anti-CD95 antibody is shown.

of peripheral T cells or the accumulation of migrated T cells from the thymus. Due to the low number of $CD4^+$ T cells in the hu-HSC NOG I-A$\beta^{-/-}$ mice that could be purified for *in vitro* experiments, we instead stimulated the whole-spleen cells from these mice with anti-CD3 and anti-CD28 antibodies *in vitro* after CFSE labeling to examine their responsiveness. The dilution of CFSE in the T-cell population was measured on days 4 and 6. The human T cells in the hu-HSC NOG I-A$\beta^{-/-}$ mice showed no significant proliferation (Fig. 9C). Thus, the human T cells that developed in the absence of I-A were also rendered unresponsive.

IgG response in hu-HSC NOG mice upon the adoptive transfer of normal T cells

Our analyses revealed that the hu-HSC NOG mice have problems in both their B-cell and T-cell populations. However, since the B cells could mount an IgG response, if not complete, to *in vitro* stimulation, we next examined whether antigen-specific IgG responses were possible *in vivo*, if supplemented with functional T cells. For this purpose, we used a TCR specific for an HA peptide ($HA_{307-319}$) that was derived from an HA-specific human T-cell clone, B16 (31). The TCR was introduced into human T cells isolated from PBMCs by retroviral vectors (Fig. 10A). The expression of the

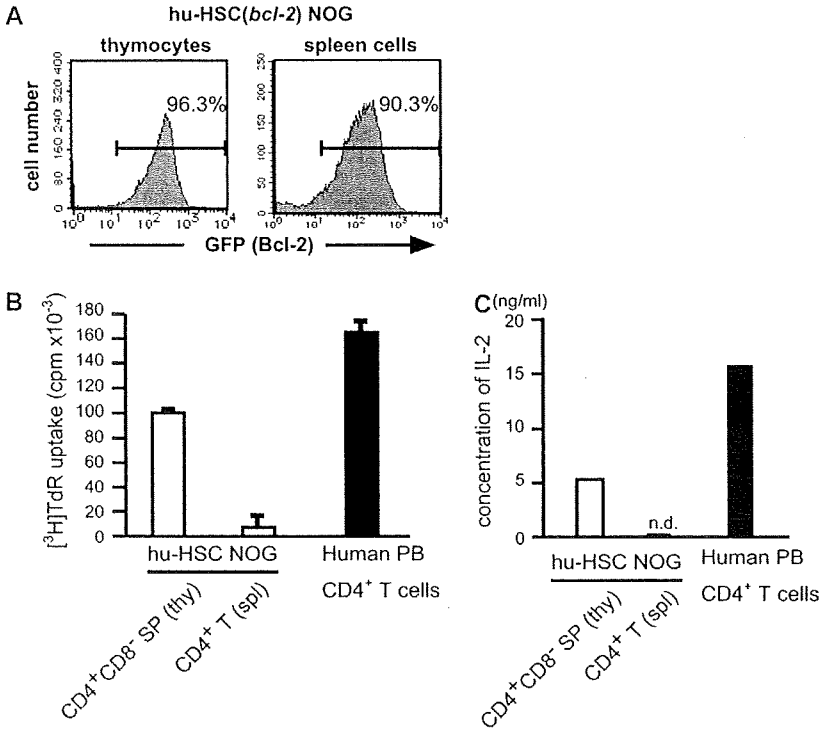

Fig. 8. Normal response of CD4$^+$CD8 SP thymocytes from hu-HSC NOG mice. (A) Reconstitution of hu-HSC (*bcl-2*) NOG mice. A representative analysis for expression of exogenous *bcl-2* represented by bicistronic GFP from retroviral vector in thymocytes and spleen cells. The thymocytes and spleen cells were prepared from the hu-HSC (*bcl-2*) NOG mice 20 weeks after reconstitution and examined the expression of GFP (n = 6). (B) Analysis of functions of human CD4$^+$CD8$^-$ SP thymocytes in hu-HSC (*bcl-2*) NOG mice *in vitro*. CD4$^+$CD8 SP thymocytes were prepared from pooled thymuses from five different hu-HSC (*bcl-2*) NOG mice grafted with the same CD34$^+$ cells (20 weeks after reconstitution). CD4$^+$ T cells were also purified from the same hu-HSC (*bcl-2*) NOG mice. These NOG-derived T cells (white bar) or normal adult peripheral blood (PB) (black bar) were stimulated with immobilized anti-CD3 and anti-CD28 antibodies. After 72-h culture, the proliferation of T cells was measured as the amounts of incorporated [^{3}H]thymidine ([^{3}H]TdR) as mentioned in Fig. 5(C). Representative data from three independent experiments are shown. (C) Quantification of IL-2 produced by human CD4$^+$CD8$^-$ SP thymocytes in hu-HSC (*bcl-2*) NOG mice *in vitro*. The amount of IL-2 in the supernatants obtained from the *in vitro* cultures described in (B) was measured by ELISA. n.d.: under detection level by ELISA.

antigen-specific TCR was also confirmed by staining with the specific tetramer (HLA-DRB1*0401/HA$_{307-319}$) (Fig. 10B). The transduced T cells produced IL-2 in response to the antigenic stimulation by a B-cell lymphoma cell line (*HLA-DRB1*0401* positive) loaded with the HA$_{307-319}$ peptide (Supplementary Figure S1, available at *International Immunology* Online). Because the B16 TCR is restricted by HLA-DR4 (DRB1*0401) and the frequency of this haplotype in the Japanese population is quite low (~1% of the population), the *HLA-DRB1*0401* gene was introduced into CD34$^+$ stem cells by retrovirus to obtain hu-HSC [HLA-DR4 (DRB1*0401)] NOG mice (Fig. 10C). We then transferred the human T cells containing the B16 TCR into the hu-HSC [HLA-DR4 (DRB1*0401)] NOG mice and immunized them with the HA$_{307-319}$ peptide (Fig. 10D). After repeating the transfer and subsequent antigenic challenges twice, we measured the amount of IgG specific for the HA peptide. Although the total IgG level in the sera was markedly elevated after immunization, the titer of HA peptide-specific IgG remained low (Fig. 10E). The increase in total IgG occurred through non-specific activation of the B-cell population by the B16 TCR-bearing human T cells, suggesting that the machinery for Ig class switch is also functional *in vivo*. We could not, however, detect any donor human T cells with the B16 TCR by staining with the specific tetramer (data not shown) 10 days after the final antigenic challenge, which may explain the absence of the HA-specific IgG response in the hu-HSC [HLA-DR4 (DRB1*0401)] NOG mice.

Discussion

In this study, we have clarified the possibilities and limitations of the present humanized mouse technology. The quasi-human immune system in humanized mice has been shown to be relatively similar to *bona fide* human immunity (5–9). However, the induction of successful immune reactions against exogenous antigens, especially the humoral responses represented by IgG responses, has been a high hurdle for humanized mice (21, 22, 24, 25). Several mechanisms have been suggested for this defect, including the skewing of human B cells toward the B-1 cell lineage (24), and the lack of interactions between B and T cells due to mismatches of the MHC (24). Our results suggest that in addition to these possibilities, other previously unrecognized mechanisms involving both B and T cells are also responsible for this limitation.

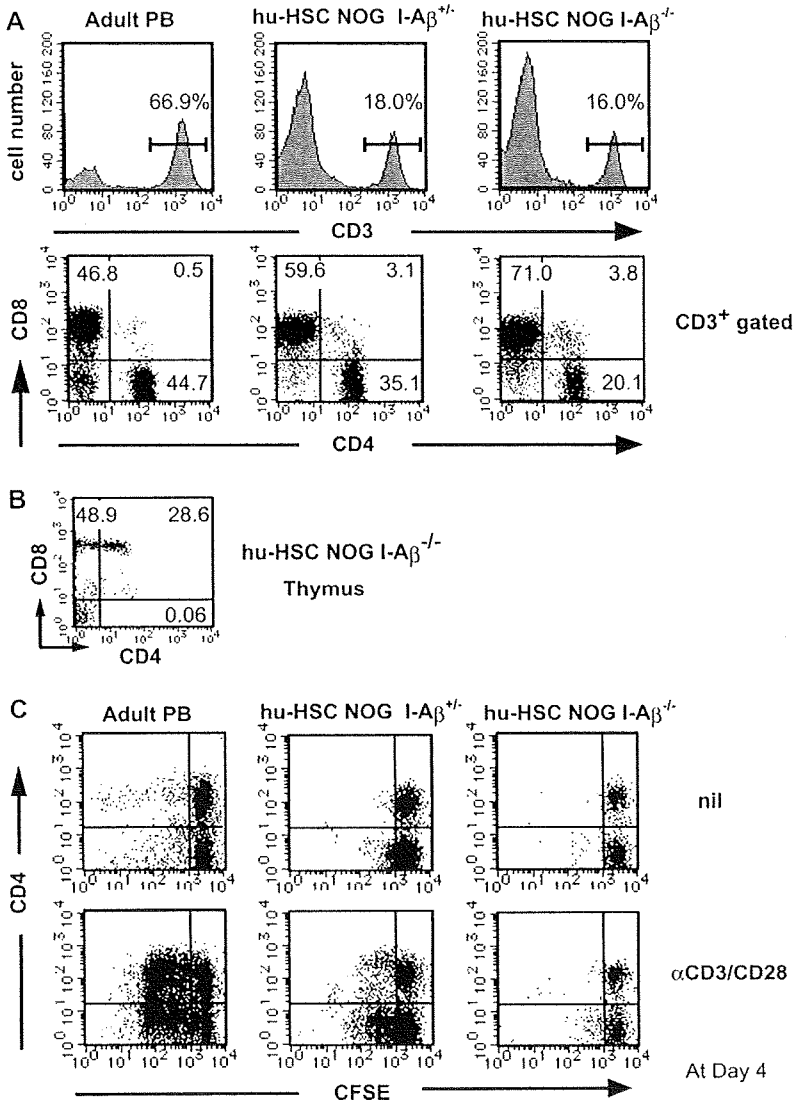

Fig. 9. Analysis of human T cells developed in hu-HSC NOG I-Aβ$^{-/-}$ mice. (A) NOG I-Aβ$^{+/-}$ or NOG I-Aβ$^{-/-}$ mice were reconstituted with human CD34$^+$ stem cells as described in Methods. Adult peripheral blood (PB) or the whole-spleen cells from respective humanized mice (20 weeks after reconstitution) were stained with anti-CD3 antibody (top panel). The CD3-positive cells were further stained with anti-CD4 and CD8 antibodies (bottom panels). A representative staining of four independent experiments is shown. (B) Development of thymocytes in hu-HSC NOG I-Aβ$^{-/-}$ mice. The pooled thymocytes from three NOG I-Aβ$^{-/-}$ mice (20 weeks after reconstitution) were stained with anti-CD4 and CD8 antibodies. (C) Analysis of functions of human CD4$^+$ T cells in the hu-HSC NOG I-Aβ$^{-/-}$ mice *in vitro*. The whole-spleen cells from the hu-HSC NOG I-Aβ$^{+/-}$ or hu-HSC NOG I-Aβ$^{-/-}$ mice (20 weeks after reconstitution) or adult PB were stained with CFSE, subsequently cultured in the presence of anti-CD3 and anti-CD28 antibodies. The cultured cells were recovered on day 4 and stained with anti-CD4 and anti-CD8 antibodies. The intensity of CFSE in CD4$^+$ or CD8$^+$ T cells was examined by FACS. A representative result from three independent experiments is shown.

The function of the 'mature' human IgD$^+$ B cells in hu-HSC NOG mice is reasonable, considering that they had an IgG response *in vitro* and *in vivo*. In contrast, there were at least three major obstacles on the T-cell side. The first was the T cells' high susceptibility to cell death. The second was their unresponsiveness, represented by their low proliferation and low production of IL-2. The third was the poor maintenance of human T cells in the mouse environment. However, several other regulatory mechanisms would be present that could also induce the loss of human T-cell function in the mouse periphery. These functional abnormalities contradict previous reports suggesting that functional human T cells develop in humanized mice, although those studies did not analyze the functions in detail (20, 22, 39, 40).

Our results using hu-HSC (*bcl-2*) NOG mice, in which the thymocytes were reactive while the splenic T cells were not, suggested that although human T cells are positively selected in the mouse thymus, they lose their function mainly in the periphery. Given the normal positive selection of human T cells in the mouse thymus, why are they compromised

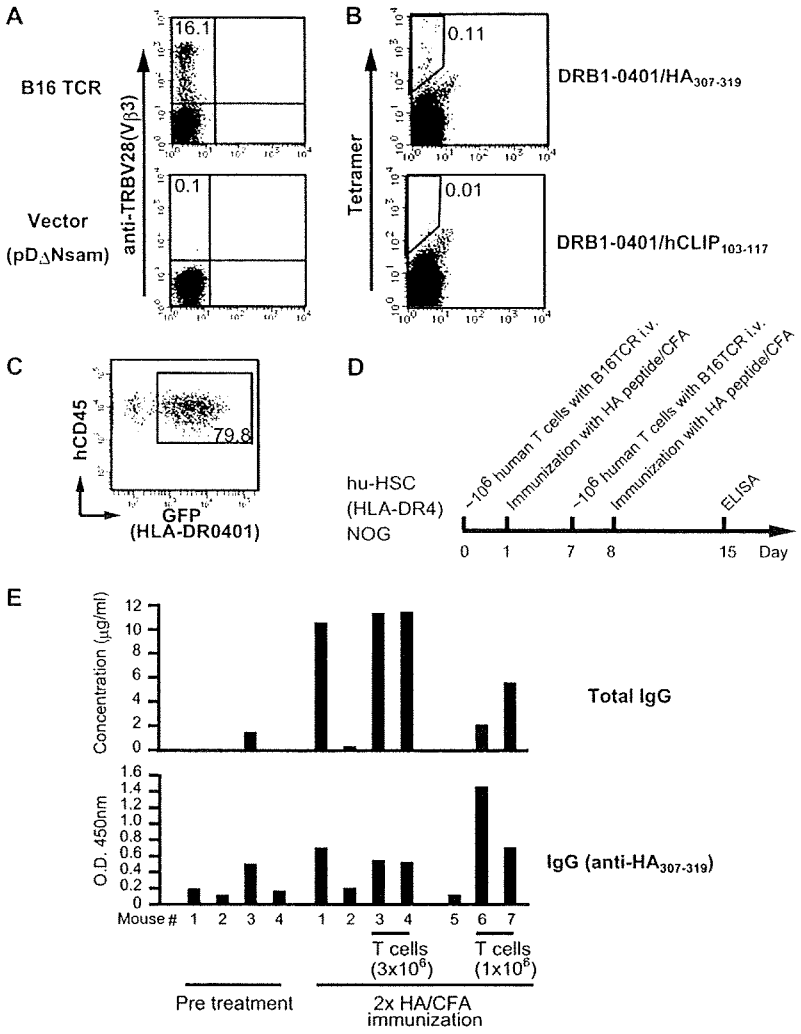

Fig. 10. Induction of IgG in hu-HSC NOG mice. (A) Retroviral delivery of $HA_{307-319}$ peptide-specific TCR (B16) into normal human T cells. Purified human T cells from normal healthy donor were activated *in vitro* as described in Methods. The T cells were subsequently spun infected with retrovirus encoding B16 TCR. The expression of B16 TCR was determined by anti-TRBV28 antibody after 10 days. (B) The frequency of the T cells with B16 TCR was further determined by staining with the specific (middle panels) or irrelevant (right panels) tetramers. (C) Reconstitution of hu-HSC [HLA-DR4 (DRB1*0401)] NOG mice. The expression of the exogenous *HLA-DRB*0401* gene in peripheral blood cells from hu-HSC [HLA-DR4 (DRB1*0401)] NOG mice was represented by bicistronic GFP from retroviral vector (8 weeks after reconstitution, $n = 6$). (D) The schema of experiments for inducing IgG in the hu-HSC [HLA-DR4 (DRB1*0401)] NOG mice upon transfer of B16 TCR-bearing human T cells. (E) Quantification of total IgG or peptide-specific IgG in the hu-HSC [HLA-DR4 (DRB1*0401)] NOG mice. One week after final antigenic challenge, the sera were collected form the mice. Total IgG (left panel) and HA-specific IgG (right panel) were measured by ELISA after 10-fold dilution of the specimens. The results from three or four different mice in each group were shown.

in the periphery? It has been controversial whether the mouse MHC on mouse thymic epithelial cells or the HLA molecules on human BM-derived cells are responsible for the thymic selection of human T cells in the hu-HSC NOG mouse. The significant delay of human T-cell development in hu-HSC NOG I-A$\beta^{-/-}$ mice suggests that the I-A on mouse epithelial cells plays a major role in the positive selection, admitting that a small number of human $CD4^+$ T cells could still develop in the absence of I-A. In this setting, there are two possibilities. The first is that human T cells are not subjected to proper negative selection by human molecules that are not present in the mouse thymus. Indeed, structural analyses of the thymus of hu-HSC NOG mice showed incomplete formation of the cortex where negative selection occurs (Supplementary Figure S2, available at *International Immunology* Online) (41). In this situation, human T cells would be inappropriately activated by I-A/human molecule-derived peptide complexes on the mouse antigen-presenting cells without the proper co-stimulations due to the barrier of species, rendering a refractory state. The second possibility is that human B cells induce unresponsiveness in the T cells because they are not professional antigen-presenting cells; that is, there is a xenoreaction to the HLA molecules on B cells by the human T cells selected by mouse MHCs.

The poor development and differentiation of human professional antigen-presenting cell like DCs and macrophages in hu-HSC NOG mice may also support this possibility (Supplementary Figure S3, available at *International Immunology* Online). The induction of the refractory state of the human T cells might be attributed to one or both of these mechanisms. As for the high susceptibility to cell death of the human T cells in hu-HSC NOG mice, a previous report suggested the high turnover of human T cells in humanized mice (42). The proliferation would be attributed, in part, to the lymphopenic situation in mouse environment where the number of human T cells is very low. Under the condition, it is possible that the human T cells in hu-HSC NOG mice become susceptible to FAS-mediated cell death (43).

The involvement of mouse I-A in the induction of the refractory state of human T cells in hu-HSC NOG mice might be tested using the hu-HSC NOG I-A$\beta^{-/-}$ mice because they developed human T cells. However, because these T cells had impaired function, the involvement of I-A remains to be determined. The results in hu-HSC NOG I-A$\beta^{-/-}$ mice might suggest that in the absence of class II on thymic epithelial cells, the positive selection of human T cells was simply incomplete or that other mechanisms were responsible for inducing abnormalities in the T cells besides the two described above. To circumvent these problems, it is necessary to construct environments in which there is no interference from mouse class II and from which a sufficient number of human T cells can still be obtained. One possibility might be to combine NOG I-A$\beta^{-/-}$ mice with BLT technology, in which an organoid consisting of pieces of fetal thymus and liver are implanted into mice with the subsequent transfer of CD34$^+$ stem cells from the same donor (44). As an alternative approach, the total replacement of mouse co-stimulatory molecules (CD80, CD86, ICAM-1, ICAM-3, etc.) and class II molecules with human orthologues might be useful.

The maintenance of human T-cell functions in the mouse environment is also important. Previous reports using hu-PBL NOD/scid mice showed that normal human T cells lose their capacity to be activated at a certain period after transplantation (45). In our study, the human T cells bearing an HA-specific TCR did not show any expansion, even after repeated immunization with the specific peptide. Supplementing the mouse model with human cytokines could be a strategy for keeping the human T cells viable and functional.

We found at least two abnormal aspects of the B-cell population in the hu-HSC NOG mice. One was a blockage of the differentiation of B cells around the transitional stage and the other was the unusual appearance of B-cell precursors in the spleen. Nevertheless, our functional analyses suggested that the differentiation and functions of the B cells were relatively close to normal. Further studies examining the B-cell function *in vivo* (e.g. expansion capacity, affinity maturation and differentiation into memory or plasma cells) must be undertaken, and additional efforts are necessary to achieve the full maturation of human B cells in mice. We believe that the hu-HSC NOG mice could be developed into a good model for studying the mechanisms involved in the proper differentiation of human B cells.

Humanized mice are becoming common tools for studying human immunity and its related diseases (46, 47). Knowledge has been accumulating about the molecular mechanisms that regulate the development and functions of hematopoietic cells in both humans and mice. It will be important to examine this information using improved model systems, for example, by creating various transgenic NOG strains that are supplemented with human cytokines or growth factors. More sophisticated humanized mice, if achieved, would lead to a better understanding of human immunity and the development of effective therapeutic treatments for human diseases involving autoimmunity or human-specific viral infections.

Supplementary data

Supplementary Figures S1–S3 are available at *International Immunology* Online.

Funding

Ministry of Education, Culture, Sports, Science and Technology of Japan and Japan Society for the Promotion of Science to K.S. (19059001) and M.I. (18100005); Takeda Scientific Foundation to T.T.

Acknowledgements

We thank K. Murata and M. Ito for the technical assistance and their secretary jobs. The authors have no financial conflict of interest.

Abbreviations

APC	allophycocyanin
BM	bone marrow
CFSE	carboxyfluorescein succinimidyl ester
CIEA	Central Institute for Experimental Animals
cμ	cytoplasmic μ chain
DC	dendritic cell
EGFP	enhanced green fluorescent protein
GAPDH	glyceraldehyde 3-phosphate dehydrogenase
HSA	human serum albumin
i.p.	intra-peritoneal
IRES	internal ribosomal entry site
i.v.	intravenous
KLH	keyhole limpet hemocyanin
KO	knockout
MACS	magnetic cell sorting
NOG	NOD/shi-scid/γc^{null}
PE	phycoerythrin
PI	propidium iodide
RT	reverse transcription
SAC	*Staphylococcus aureus* cowan
SP	single positive
TCR	T-cell receptor
γc	γ chain

References

1 Grabstein, K. H., Waldschmidt, T. J., Finkelman, F. D. *et al.* 1993. Inhibition of murine B and T lymphopoiesis *in vivo* by an anti-interleukin 7 monoclonal antibody. *J. Exp. Med.* 178:257.
2 Dittel, B. N. and LeBien, T. W. 1995. The growth response to IL-7 during normal human B cell ontogeny is restricted to B-lineage cells expressing CD34. *J. Immunol.* 154:58.
3 Leonard, W. J., Shores, E. W. and Love, P. E. 1995. Role of the common cytokine receptor gamma chain in cytokine signaling and lymphoid development. *Immunol. Rev.* 148:97.

4 Schraven, B. and Kalinke, U. 2008. CD28 superagonists: what makes the difference in humans? *Immunity* 28:591.
5 Shultz, L. D., Ishikawa, F. and Greiner, D. L. 2007. Humanized mice in translational biomedical research. *Nat. Rev. Immunol.* 7:118.
6 Manz, M. G. 2007. Human-hemato-lymphoid-system mice: opportunities and challenges. *Immunity* 26:537.
7 Legrand, N., Weijer, K. and Spits, H. 2006. Experimental models to study development and function of the human immune system *in vivo*. *J. Immunol.* 176:2053.
8 Payne, K. J. and Crooks, G. M. 2007. Immune-cell lineage commitment: translation from mice to humans. *Immunity* 26:674.
9 Macchiarini, F., Manz, M. G., Palucka, A. K. and Shultz, L. D. 2005. Humanized mice: are we there yet? *J. Exp. Med.* 202:1307.
10 Manning, D. D., Reed, N. D. and Shaffer, C. F. 1973. Maintenance of skin xenografts of widely divergent phylogenetic origin of congenitally athymic (nude) mice. *J. Exp. Med.* 138:488.
11 McCune, J. M., Namikawa, R., Kaneshima, H., Shultz, L. D., Lieberman, M. and Weissman, I. L. 1988. The SCID-hu mouse: murine model for the analysis of human hematolymphoid differentiation and function. *Science* 241:1632.
12 Shultz, L. D., Schweitzer, P. A., Christianson, S. W. *et al.* 1995. Multiple defects in innate and adaptive immunologic function in NOD/LtSz-scid mice. *J. Immunol.* 154:180.
13 Pflumio, F., Lapidot, T., Murdoch, B., Patterson, B. and Dick, J. E. 1993. Engraftment of human lymphoid cells into newborn SCID mice leads to graft-versus-host disease. *Int. Immunol.* 5:1509.
14 Huppes, W., De Geus, B., Zurcher, C. and Van Bekkum, D. W. 1992. Acute human vs. mouse graft vs. host disease in normal and immunodeficient mice. *Eur. J. Immunol.* 22:197.
15 Larochelle, A., Vormoor, J., Hanenberg, H. *et al.* 1996. Identification of primitive human hematopoietic cells capable of repopulating NOD/SCID mouse bone marrow: implications for gene therapy. *Nat. Med.* 2:1329.
16 Ito, M., Hiramatsu, H., Kobayashi, K. *et al.* 2002. NOD/SCID/gamma(c)(null) mouse: an excellent recipient mouse model for engraftment of human cells. *Blood* 100:3175.
17 DiSanto, J. P., Muller, W., Guy-Grand, D., Fischer, A. and Rajewsky, K. 1995. Lymphoid development in mice with a targeted deletion of the interleukin 2 receptor gamma chain. *Proc. Natl Acad. Sci. USA* 92:377.
18 Cao, X., Shores, E. W., Hu-Li, J. *et al.* 1995. Defective lymphoid development in mice lacking expression of the common cytokine receptor gamma chain. *Immunity* 2:223.
19 Ohbo, K., Suda, T., Hashiyama, M. *et al.* 1996. Modulation of hematopoiesis in mice with a truncated mutant of the interleukin-2 receptor gamma chain. *Blood* 87:956.
20 Shultz, L. D., Lyons, B. L., Burzenski, L. M. *et al.* 2005. Human lymphoid and myeloid cell development in NOD/LtSz-scid IL2R gamma null mice engrafted with mobilized human hemopoietic stem cells. *J. Immunol.* 174:6477.
21 Ishikawa, F., Yasukawa, M., Lyons, B. *et al.* 2005. Development of functional human blood and immune systems in NOD/SCID/IL2 receptor {gamma} chain(null) mice. *Blood* 106:1565.
22 Traggiai, E., Chicha, L., Mazzucchelli, L. *et al.* 2004. Development of a human adaptive immune system in cord blood cell-transplanted mice. *Science* 304:104.
23 Hiramatsu, H., Nishikomori, R., Heike, T. *et al.* 2003. Complete reconstitution of human lymphocytes from cord blood CD34+ cells using the NOD/SCID/gammacnull mice model. *Blood* 102:873.
24 Matsumura, T., Kametani, Y., Ando, K. *et al.* 2003. Functional CD5+ B cells develop predominantly in the spleen of NOD/SCID/gammac(null) (NOG) mice transplanted either with human umbilical cord blood, bone marrow, or mobilized peripheral blood CD34+ cells. *Exp. Hematol.* 31:789.
25 Baenziger, S., Tussiwand, R., Schlaepfer, E. *et al.* 2006. Disseminated and sustained HIV infection in CD34+ cord blood cell-transplanted Rag2-/-gamma c-/- mice. *Proc. Natl Acad. Sci. USA* 103:15951.
26 Cosgrove, D., Gray, D., Dierich, A. *et al.* 1991. Mice lacking MHC class II molecules. *Cell* 66:1051.
27 Suemizu, H., Yagihashi, C., Mizushima, T. *et al.* 2008. Establishing EGFP congenic mice in a NOD/Shi-scid IL2Rg(null) (NOG) genetic background using a marker-assisted selection protocol (MASP). *Exp. Anim.* 57:471.
28 Tsuganezawa, K., Kiyokawa, N., Matsuo, Y. *et al.* 1998. Flow cytometric diagnosis of the cell lineage and developmental stage of acute lymphoblastic leukemia by novel monoclonal antibodies specific to human pre-B-cell receptor. *Blood* 92:4317.
29 Kaneko, S., Onodera, M., Fujiki, Y., Nagasawa, T. and Nakauchi, H. 2001. Simplified retroviral vector gcsap with murine stem cell virus long terminal repeat allows high and continued expression of enhanced green fluorescent protein by human hematopoietic progenitors engrafted in nonobese diabetic/severe combined immunodeficient mice. *Hum. Gene Ther.* 12:35.
30 Morita, S., Kojima, T. and Kitamura, T. 2000. Plat-E: an efficient and stable system for transient packaging of retroviruses. *Gene Ther.* 7:1063.
31 Gebe, J. A., Novak, E. J., Kwok, W. W., Farr, A. G., Nepom, G. T. and Buckner, J. H. 2001. T cell selection and differential activation on structurally related HLA-DR4 ligands. *J. Immunol.* 167:3250.
32 Simmons, A. and Jantz, K. 2006. Use of a lentivirus/VSV pseudotype virus for highly efficient genetic redirection of human peripheral blood lymphocytes. *Nat. Protoc.* 1:2688.
33 Sims, G. P., Ettinger, R., Shirota, Y., Yarboro, C. H., Illei, G. G. and Lipsky, P. E. 2005. Identification and characterization of circulating human transitional B cells. *Blood* 105:4390.
34 Imamura, R., Miyamoto, T., Yoshimoto, G. *et al.* 2005. Mobilization of human lymphoid progenitors after treatment with granulocyte colony-stimulating factor. *J. Immunol.* 175:2647.
35 Hystad, M. E., Myklebust, J. H., Bo, T. H. *et al.* 2007. Characterization of early stages of human B cell development by gene expression profiling. *J. Immunol.* 179:3662.
36 Leonard, W. J. and Spolski, R. 2005. Interleukin-21: a modulator of lymphoid proliferation, apoptosis and differentiation. *Nat. Rev. Immunol.* 5:688.
37 Ozaki, K., Spolski, R., Ettinger, R. *et al.* 2004. Regulation of B cell differentiation and plasma cell generation by IL-21, a novel inducer of Blimp-1 and Bcl-6. *J. Immunol.* 173:5361.
38 Choi, E. Y., Jung, K. C., Park, H. J. *et al.* 2005. Thymocyte-thymocyte interaction for efficient positive selection and maturation of CD4 T cells. *Immunity* 23:387.
39 Yahata, T., Ando, K., Nakamura, Y. *et al.* 2002. Functional human T lymphocyte development from cord blood CD34+ cells in nonobese diabetic/Shi-scid, IL-2 receptor gamma null mice. *J. Immunol.* 169:204.
40 Saito, Y., Kametani, Y., Hozumi, K. *et al.* 2002. The *in vivo* development of human T cells from CD34(+) cells in the murine thymic environment. *Int. Immunol.* 14:1113.
41 McCaughtry, T. M., Baldwin, T. A., Wilken, M. S. and Hogquist, K. A. 2008. Clonal deletion of thymocytes can occur in the cortex with no involvement of the medulla. *J. Exp. Med.* 205:2575.
42 Legrand, N., Cupedo, T., van Lent, A. U. *et al.* 2006. Transient accumulation of human mature thymocytes and regulatory T cells with CD28 superagonist in "human immune system" Rag2(-/-) gammac(-/-) mice. *Blood* 108:238.
43 Fortner, K. A. and Budd, R. C. 2005. The death receptor Fas (CD95/APO-1) mediates the deletion of T lymphocytes undergoing homeostatic proliferation. *J. Immunol.* 175:4374.
44 Melkus, M. W., Estes, J. D., Padgett-Thomas, A. *et al.* 2006. Humanized mice mount specific adaptive and innate immune responses to EBV and TSST-1. *Nat. Med.* 12:1316.
45 Tary-Lehmann, M., Lehmann, P. V., Schols, D., Roncarolo, M. G. and Saxon, A. 1994. Anti-SCID mouse reactivity shapes the human CD4+ T cell repertoire in hu-PBL-SCID chimeras. *J. Exp. Med.* 180:1817.
46 Yajima, M., Imadome, K., Nakagawa, A. *et al.* 2008. A new humanized mouse model of Epstein-Barr virus infection that reproduces persistent infection, lymphoproliferative disorder, and cell-mediated and humoral immune responses. *J. Infect. Dis.* 198:673.
47 Kumar, P., Ban, H. S., Kim, S. S. *et al.* 2008. T cell-specific siRNA delivery suppresses HIV-1 infection in humanized mice. *Cell* 134:577.

Highly Sensitive Model for Xenogenic GVHD Using Severe Immunodeficient NOG Mice

Ryoji Ito, Ikumi Katano, Kenji Kawai, Hiroshi Hirata, Tomoyuki Ogura, Tsutomu Kamisako, Tomoo Eto, and Mamoru Ito

Background. Several animal models for xenogenic (xeno) graft versus host disease (GVHD) have been developed in immunodeficient mice, such as C.B-17-*scid* and nonobese diabetes (NOD)/severe combined immunodeficiency (SCID), by human peripheral blood mononuclear cell (hPBMC) transplantation. However, these models pose problems because they require sublethal total body irradiation of the mice and a large number of hPBMCs to induce GVHD, and the timing of onset of GVHD is also unstable. The aim of this study is to establish improved murine models of xeno-GVHD using novel immunodeficient NOD/Shi-*scid* IL2rγ^{null} (NOG) mice.

Methods. In three strains of immunodeficient mice, NOG, BALB/cA-RAG2^{null} IL2rγ^{null}, and NOD/SCID mice, GVHD was induced by transplantation of hPBMCs with or without total body irradiation, and the GVHD symptoms in these strains were compared.

Results. After intravenous transplantation of hPBMCs, NOG mice showed early onset of GVHD symptoms and a small number of hPBMCs (2.5×10^6) was sufficient to induce GVHD when compared with BALB/cA-RAG2^{null} IL2rγ^{null} and NOD/SCID mice. In addition, total body irradiation was not always necessary in the present model.

Conclusions. These results indicate that our model using the NOG mouse is a useful tool to investigate GVHD and to develop effective drugs for GVHD.

Keywords: Xeno-GVHD, Immunodeficient mice, Model animals.

(*Transplantation* 2009;87: 1654–1658)

Graft versus host disease (GVHD) is known as a major complication in allogenic bone marrow (BM) transplantation for therapy of several diseases such as acute/chronic leukemia, aplastic anemia, and congenital immunodeficiency, and is characterized by high mortality after onset. In the recipients, severe damage by donor lymphocyte infusion is generally observed in various organs including the liver, skin, lungs, kidneys, and intestine (*1*). However, there is no effective treatment for this disease to date.

Xenograft model animals using immunodeficient mice have been used for medical research on various human diseases. Severe combined immunodeficient mice (C.B-17-*scid*) discovered by Bosma et al. (*2*), lack functional T and B lymphocytes, and thus provided a first model termed "SCID-hu" by reconstitution with human peripheral blood mononuclear cells (hPBMC) or fetal lymphoid tissues in these mice (*3–8*). However, even in C.B-17-*scid* mice, only a low level of human cells was reconstituted because of the remaining host innate immune system. Nonobese diabetes (NOD)/SCID mice that were modified from C.B-17-*scid* mice are better recipients for engraftment of hPBMC than C.B-17-*scid* mice, probably because of reduced levels of natural killer (NK) cell activity and additional deficiencies in innate immunity (*9, 10*). In fact, in vivo depletion of NK cells in C.B-17-*scid* or NOD/SCID mice by treatment with NK cell-specific antibodies (e.g., anti-asialo-GM1, anti-TM-β1, and anti-NK1.1) resulted in significantly higher engraftment rates of reconstituted human cells (*11, 12*). However, these models still have several problems including the need for sublethal total body irradiation, and the large number of hPBMCs required to induce GVHD, and instability in the timing of onset of GVHD symptoms. In addition, intravenous transplantation of hPBMCs into these animals failed to induce GVHD (*13*). In clinical cases, the cell transfer route is actually restricted through veins but not through the peritoneal cavity in the therapy for BM transplantation. In this sense, the possibility of intravenous transplantation of hPBMCs may be an important issue for xeno-GVHD animal models.

Van Rijn et al. (*14*) reported a new model using H-2^d-RAG2^{null} IL2rγ^{null} mice lacking T, B, and NK cells. This model has advantages compared with NOD/SCID mice, including no leaky lymphocytes or lymphoid tumor formation, and higher engraftment of human T cells than in previous xeno-GVHD

This work was supported by a Grant-in-Aid for Scientific Research (S) from the Ministry of Education, Culture, Sports, Science and Technology (MEXT) of Japan.

Departments of Laboratory Animal Research, Animal Resources Management, and Pathology Research, Central Institute for Experimental Animals, Miyamae, Kawasaki, Japan.

Address correspondence to: Ryoji Ito, Med.Sci., Central Institute for Experimental Animals, 1430 Nogawa, Miyamae, Kawasaki 216-0001, Japan.

E-mail: rito@ciea.or.jp

Received 29 December 2008. Revision requested 20 January 2009.

Accepted 9 March 2009.

ISSN 0041-1337/09/8711-1654

DOI: 10.1097/TP.0b013e3181a5cb07

models. However, this model still has disadvantages because a large number of hPBMCs (3×10^7 cells) and total body irradiation are required to induce GVHD.

NOD/Shi-*scid* IL2rγ^{null} (NOG) mice were recently established by introduction of the interleukin (IL)-2rγ-targeted gene of IL-2rγ KO mice (*15*) by nine backcross matings of IL-2rγ KO mice to NOD/SCID mice. They showed an extremely high engraftment rate of transplanted human cells compared with other immunodeficient mice because of their higher immunodeficiency, that is, the lack of T, B, and NK cells, and reduced functions of macrophage and dendritic cells. Therefore, they are known an excellent model of "humanized mice" where human cells are well developed and differentiated after transfer of human cord blood $CD34^+$ cells (*16–18*).

This study reported a novel xeno-GVHD animal model using these NOG mice, in which the model showed earlier onset of GVHD symptoms by intravenous transfer of hPBMCs.

MATERIALS AND METHODS

Mice

NOG (formal name, NOD.Cg-*prkdc*^{scid}*il2rg*^{tm1Sug}/Jic) and BALB/cA-RAG2^{null} IL2rγ^{null} (RAG2^{null} IL2rγ^{null}; formal name, C.Cg-*rag2*^{tm1Fwa}*il2rg*^{tm1Sug}/AJic) mice were bred and maintained under specific pathogen-free conditions in the Central Institute for Experimental Animals. NOD.CB17-*prkdc*^{scid}/ShiJic (NOD/SCID) mice were purchased from CIEA Japan Inc. (Tokyo, Japan). Mice were housed in sterilized cages and fed sterilized food and water. These three strains of immunodeficient mice were used at the age of 8 to 10 weeks. In most experiments, NOG mice were irradiated with 2.5 Gy, whereas RAG2^{null} IL2rγ^{null} and NOD/SCID mice were irradiated with 3.5 Gy using an X-ray system (MBR-1505R, Hitachi Medical Corp., Tokyo, Japan) 1 day before hPBMC transplantation.

All animal experiments were approved by the Institutional Animal Care and Use Committee and were performed in accordance with Central Institute for Experimental Animal guidelines.

Transplantation of hPBMCs

Human peripheral blood (PB) was obtained from healthy volunteers with their consent and hPBMCs were isolated by a Ficoll-Hypaque (GE Healthcare UK Ltd., England) density centrifugation and washed in phosphate-buffered saline (PBS). Cells were resuspended in PBS and injected through the peritoneal cavity or tail vein into the irradiated or nonirradiated mice. Body weights of all mice were obtained at twice weekly.

Flow Cytometry

PB and spleens were obtained from mice transplanted with hPBMCs and were prepared as single-cell suspensions. Cells were incubated for 30 min at 4°C under protection from light with a mixture of appropriate fluorescently labeled monoclonal antibodies. After washing with PBS containing 1% fetal calf serum, the cells were suspended in propidium iodide solution (Becton Dickinson, BD Biosciences, San José, CA), followed by multicolor flow cytometry with FACS Canto (Becton Dickinson) and analysis by FACS Diva software (Becton Dickinson). The engraftment rates of human cells were expressed as the percentage of human $CD45^+$ cells in total cells. The antibodies used for recognition of the cell surface molecules were anti-human CD45-fluorescein isothiocyanate (FITC, Becton Dickinson) and human CD3-phycoerythrin-Cy7 (PE-Cy7, Beckman Coulter, Inc., CA).

Immunohistochemistry

For immunohistochemistry, liver, lungs, and kidneys from mice transplanted with hPBMCs were fixed with 10% buffered formalin and embedded in paraffin. Sections of 5-μm thick were placed on amino-silane coated glass slides (Matsunami Glass, Osaka, Japan) and were immunostained by the universal immunoenzyme polymer method (Nichirei, Tokyo, Japan). After deparaffinization, sections were incubated with anti-human CD45 monoclonal antibodies (Dako Cytomation, Glostrup, Denmark) overnight at 4°C and were serially incubated with peroxidase-labeled polymer conjugated goat anti-mouse antibody (Histofine Simplestain Max-PO; Nichirei, Tokyo, Japan) for 30 min at room temperature. For color development, these sections were incubated with 0.02% 3,3′-diaminobenzidine (DAB, Dojindo, Kumamoto, Japan) substrate solution containing 0.006% H_2O_2. Immunostained sections were counterstained with hematoxylin for visualization of nuclei.

RESULTS

Induction of GVHD in NOG Mice

To investigate the appropriate route and minimum cell count of hPBMC to induce xeno-GVHD, various numbers of hPBMCs were transferred into irradiated NOG mice by intravenous or intraperitoneal routes (Table 1). On administration of 10×10^6 hPBMCs by the intraperitoneal route, all NOG mice died within 1 month, and 70% (seven of ten) of NOG mice survived for longer than 2 months when 5×10^6 hPBMCs were transplanted. When 5×10^6 or 10×10^6 hPBMCs were transplanted by the intravenous route, all NOG mice died approximately 1 month or 2 weeks earlier than by the intraperitoneal route. In the next experiment, three different counts of hPBMCs (5×10^6, 2.5×10^6, or 1×10^6) were intravenously administered to irradiated three NOG mice each for induction of GVHD (Table 2). NOG mice transplanted with 5×10^6 and 2.5×10^6 hPBMCs died within 1 to 1.5 months after cell transfer. In contrast, all NOG mice transplanted with 1×10^6 cells survived for longer than 3 months. These results demonstrated that the intravenous route was more effective for GVHD induction than the intraperitoneal one, and at least 2.5×10^6 cells are necessary to induce GVHD in NOG mice.

TABLE 1. Comparison of transplantation routes for induction of GVHD in NOG mice

Route of transplantation	Cell numbers of PBMC transferred	Numbers of mice dying from GVHD	Mean days until death
IP	5×10^6	7/10	40.4±9.0
	10×10^6	4/4	23.3±9.7
IV	5×10^6	11/11	26.9±14.6
	10×10^6	8/8	14.5±1.4

IP, intraperitoneal inoculation; IV, intravenous inoculation; GVHD, graft versus host disease; NOG, NOD/Shi-*scid* IL2rγ^{null}; PBMC, peripheral blood mononuclear cell.

TABLE 2. Minimum cell numbers for induction of GVHD in NOG mice

Cell numbers of PBMC transferred	Numbers of mice dying from GVHD	Mean days until death
5×10^6	3/3	34.7±6.7
2.5×10^6	3/3	46.3±14.3
1×10^6	0/3	—

GVHD, graft versus host disease; NOG, NOD/Shi-*scid* IL2rγ^{null}; PBMC, peripheral blood mononuclear cell.

Comparison of Xeno-GVHD Symptoms Among Different Strains of Immunodeficient Mice

To verify the usefulness of NOG mice as a model of xeno-GVHD, we compared the onset and symptoms of xeno-GVHD among three strains of immunodeficient mice, NOG, RAG2^{null} IL2rγ^{null}, and NOD/SCID, that were transplanted with 10×10^6 hPBMCs with or without irradiation (Fig. 1). In transplantation after irradiation, all NOG and RAG2^{null} IL2rγ^{null} mice died at 2 weeks and at 1 to 2 months, respectively, with reduction of body weight in a time dependent manner. In contrast, NOD/SCID mice survived for longer than 2 months without reduced body weight (Fig. 1A). Surprisingly, all NOG mice also died at 1.5 to 2.5 months after transplantation with the same numbers (10×10^6) of hPBMCs without irradiation, but all NOD/SCID and RAG2^{null} IL2rγ^{null} mice survived for more than 3 months (Fig. 1B). These results indicate that NOG mice showed earlier onset of GVHD symptoms and uniformly died when compared with NOD/SCID and RAG2^{null} IL2rγ^{null} mice. In addition, total body irradiation was not necessary for induction of xeno-GVHD only in NOG mice when 10×10^6 hPBMCs were transplanted.

Human Cell Engraftment in Xeno GVHD-Induced Mice

At 2 weeks after transplantation of 5×10^6 hPBMCs through the tail vein of three strains of irradiated immunodeficient mice, we isolated mononuclear cells from PB, BM, and spleen and analyzed engraftment rates of human CD45$^+$ leukocytes by flow cytometry. As shown in Figure 2, the engraftment rates of human CD45$^+$ cells increased more dramatically in PB, BM, and spleens of NOG mice than in those of RAG2^{null} IL2rγ^{null} and NOD/SCID mice. Low rates of engraftment of human CD45$^+$ cells were observed in the spleen from RAG2^{null} IL2rγ^{null} mice but not in NOD/SCID mice. Only a few human CD45$^+$ cells were present in BM and PB of RAG2^{null} IL2rγ^{null} and NOD/SCID mice. The engrafted human CD45$^+$ cells observed in these immunodeficient mice were almost all CD3$^+$ cells (data not shown). These findings suggested that severe GVHD symptoms in NOG mice were caused by higher engraftment of human T cells.

Infiltration of Human Cells in Various Organs

To investigate the infiltration of human lymphocytes into nonlymphoid tissues in xeno GVHD-induced mice, we performed immunohistochemical analysis of the liver, lungs, and kidneys from three strains of irradiated and 5×10^6 hPBMCs transplanted immunodeficient mice using an anti-human CD45 antibody. As seen in Figure 3, remarkably abundant invasion of human CD45$^+$ cells was observed around the veins in the liver, lungs, and kidneys of NOG mice, whereas only a few human CD45 cells were observed in the liver and lungs, and none in the kidneys of RAG2^{null} IL2rγ^{null} and NOD/SCID mice.

DISCUSSION

In present study, we reported a novel model for xeno-GVHD using NOG mice. This model showed significantly rapid onset of GVHD and uniform death after cell transfer when compared with RAG2^{null} IL2rγ^{null} and NOD/SCID models. It also had several advantages over other immunodeficient mice, in that intravenous transplantation was possible, a small number of hPBMCs (2.5×10^6) was sufficient to induce GVHD, and total body irradiation was not always necessary. In previous reports, GVHD was induced effectively by transplantation of PBMCs only by the intraperitoneal route and not by the intravenous route, when xeno GVHD models of SCID or NOD/SCID mice were used. Interestingly, intravenous transplantation could easily induce xeno GVHD in

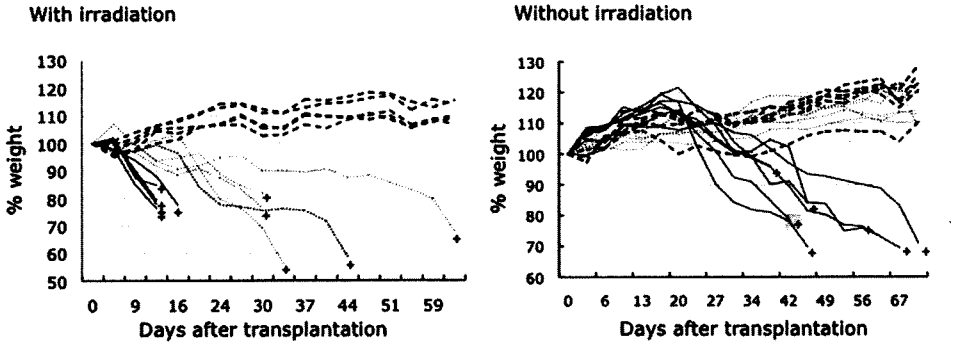

FIGURE 1. Induction of xenogenic graft versus host disease (GVHD) in NOD/Shi-*scid* IL2rγ^{null} (NOG), RAG2^{null} IL2rγ^{null}, and non-obese diabetes (NOD)/severe combined immunodeficiency (SCID) mice. After irradiation (NOG: 2.5 Gy, RAG2^{null} IL2rγ^{null} and NOD/SCID: 3.5 Gy) and after intravenous transplantation of 10×10^6 human peripheral blood mononuclear cells, all mice were weighed twice weekly. All NOG mice died from GVHD with (*left*; n=5) or without (*right*; n=7) irradiation earlier than other immunodeficient mice. All irradiated RAG2^{null} IL2rγ^{null} mice (n=5) died after 1 to 2 months, whereas all nonirradiated mice (n=7) survived for more than 2 months. NOD/SCID mice with or without irradiation (n=5 or n=7) did not die for more than 2 months. Three different *lines* indicate NOG (*solid lines*), RAG2^{null} IL2rγ^{null} (*dotted lines*) and NOD/SCID (*bold dotted lines*); + indicates death of the mouse, and % weight shows weight change percentage from the initial weight.